Journal of Vertebrate Paleontology 24(3):591–609, September 2004

MORPHOMETRIC ANALYSIS OF EVOLUTIONARY TRENDS IN THE CERATOPSIAN POSTCRANIAL SKELETON

BRENDA CHINNERY*
Museum of the Rockies, Montana State University, 600 W. Kagy Blvd., Bozeman, MT 59717, bchinnery@montana.edu

ABSTRACT—The cranial anatomy of ceratopsian ("horned") dinosaurs is well understood, but the postcranial skeleton has been largely ignored in previous studies of phylogeny, evolution, and function. In order to study morphological differences among ceratopsian postcranial elements and to compare evolutionary patterns, multivariate (Principal Components Analysis) and bivariate methods were used to analyze linear measurement data, and the shape methods Resistant-Fit Theta-Rho Analysis (RFTRA), Least-Squares Theta-Rho Analysis (LSTRA), and Euclidean Distance Matrix Analysis (EDMA) were applied to biological landmark data. Results of the analyses show that size is the primary change through ceratopsian skeleton evolution. Elements display positive allometry, and increasing structural support is evident, especially in the radius and fibula.

Phylogenetic distribution of ceratopsian postcrania agrees with the skull material included in recent cladistic analyses. *Psittacosaurus* elements are in many ways derived relative to those of non-ceratopsid neoceratopsians, and evidence suggests that *Psittacosaurus* was bipedal, while non-ceratopsid neoceratopsians were not, except maybe for *Udanoceratops*. With increasing body size, neoceratopsian limbs bowed laterally.

The variety of methods allows for unbiased interpretation of results, provides more information than any one method, and provides controls for each other. However, sample sizes are not ideal, and all results should be treated with caution at this time.

INTRODUCTION

Ceratopsia are a clade of ornithischian dinosaurs comprised of the family Psittacosauridae and the infraorder Neoceratopsia (Sereno, 1984, 1986, 1990; Dodson and Currie, 1990). Although the oldest ceratopsians known may have lived as early as the Early Cretaceous (*Chaoyangsaurus*; Zhao et al., 1999), the clade is mainly known from the radiations that occurred during the middle and Late Cretaceous of Asia and the Late Cretaceous of the western United States and Canada.

Ceratopsian postcranial anatomy varies throughout the clade. Psittacosauridae, a clade of small herbivores known only from the Early Cretaceous of Asia, share the diagnostic ceratopsian rostral bone with the other members of Ceratopsia. Psittacosaurs are characterized by long hind limb elements, relatively short forelimb elements, and a reduced manus (Sereno, 1990), suggesting that members of this clade were facultatively bipedal. Psittacosaurids are relatively small dinosaurs, not more than two meters in length.

Neoceratopsia (Ceratopsia excluding Psittacosauridae; Sereno, 1984, 1986) comprise the majority of Ceratopsia. These dinosaurs first appeared in the Early Cretaceous of Asia as small, possibly bipedal herbivores, and over time evolved into large-bodied graviportal quadrupeds. Basal neoceratopsians vary in morphology, continental distribution, and fossil age. The group is paraphyletic (Sereno, 1986, 2000; Chinnery and Weishampel, 1998), consisting of taxa more closely related to the ceratopsids of North America. Ceratopsidae are a monophyletic clade comprised of two subfamilies, Centrosaurinae and Chasmosaurinae. Postcranially these subfamilies have been considered extremely similar (Dodson and Currie, 1990). All are robust quadrupeds, and the functional changes associated with this graviportal lifestyle were thought to be indistinct at the subfamilial level and even less distinct among genera within the subfamilies.

The present study of ceratopsian postcranial anatomy involves the application of morphometric analyses treated in a phylogenetic context. This project was conceived with the realization of how essential it is that we understand the evolution and growth of the ceratopsian postcranial skeleton, because it comprises the majority of the skeletal mass, is responsible for stature and locomotion (among other functions), and evolved through time along with the cranial skeleton. The postcranial skeleton has been neglected in the past because phylogenetic analyses have relied primarily on cranial characters (Sereno, 1984, 1986, 2000; Chinnery and Weishampel, 1998; Makovicky, 2002; Dodson et al., in press). The postcranial skeleton is not only important for phylogenetic analysis, but also for any discussions of function, behavior, or growth within the clade.

Linear measurement and landmark data are available in the Supplemental Materials (see Appendix) online at: http://www.vertpaleo.org/jvp/JVPcontents.html, as are additional results and text not able to be included here. Girdle and limb elements of all available ceratopsian taxa were compared at subfamial and generic levels. Only the former is included in this paper, because comparisons of taxa at the generic level are simply too long to include. However, they are available in the Supplemental Materials. Additional objectives of the project were to document and describe taxonomic differences in the ceratopsian postcranial skeleton and to compare growth changes to evolutionary changes in postcranial skeletal anatomy. The application of a variety of morphometric techniques ensures relatively non-biased results and provides quantified and testable results as well as data for inclusion in future analyses.

Morphometry consists of techniques used to capture the shape and size of an object (usually, but not always, biological), which can then be compared with another object. The techniques have evolved through time from the deformation grids of D'Arcy Thompson (1917) to the myriad methods used today (e.g., Chapman, 1990 and references therein; Richtsmeier et al., 1992; Chinnery and Chapman, 1998). As an organism develops, stresses including gravity, movement, posture, and growth cause changes in shapes and sizes of skeletal (and soft tissue) elements. Such changes are often subtle and may be missed without the use of morphometrics. Quantitative approaches have been used to capture and clarify evolutionary changes in both living and extinct organisms, as well as to provide the means to study sexual dimorphism, posture, and locomotor changes ontogenetically and

* Present address: 1620 Green Meadow Lane, Spring Branch, Texas 78070.

phylogenetically, and to identify heterochronic processes (e.g., references in Chapman, 1990). These methods provide a powerful means to study growth, skeletal evolution, and function, which is the reason for applying them to the study of ceratopsian postcrania.

Current phylogenies of neoceratopsians (Makovicky, 2002) and ceratopsids (Dodson et al., in press) provide the baseline for the comparisons in this project. For placement of postcranial attributes, these two trees have been combined into a composite tree (Fig. 1). Neither of the original trees is disrupted, but the resulting tree is not a true tree in the cladistic sense. The basic tree topology includes Pachycephalosauria as the outgroup to Ceratopsia. Ceratopsia include Psittacosauridae and Neoceratopsia. Neoceratopsia are comprised of Ceratopsidae and a paraphyletic assemblage of basal forms.

Institutional Abbreviations—**AMNH**, American Museum of Natural History, New York; **ANSP**, Academy of Natural Sciences of Philadelphia; **BHI**, Black Hills Institute, South Dakota; **CM**, Carnegie Museum, Pittsburgh; **DMNH**, Denver Museum of Nature and Science, Colorado; **GPM**, Glenrock Paleontology Museum, Wyoming; **KUVP**, Kansas University Vertebrate Paleontology; **MCZ**, Museum of Comparative Zoology, Massachusetts; **MNA**, Museum of Northern Arizona, Flagstaff; **MOR**, Museum of the Rockies, Montana; **NMC**, Canadian Museum of Nature, Ontario; **NMMNH**, New Mexico Museum of Natural History, Albuquerque; **OMNH**, Oklahoma Museum of Natural History; **PIN**, Paleontological Institute, Russian Academy of Sciences, Moscow; **ROM**, Royal Ontario Museum, Toronto; **RTMP**, Royal Tyrrell Museum of Palaeontology, Canada; **TCM**, The Children's Museum of Indianapolis; **TMM**, Texas Memorial Museum, Austin; **UCM**, University of Colorado Museum, Boulder; **UCMP**, University of California Museum of Paleontology, Berkeley; **USNM**, United States National Museum, Washington DC; **UTEP**, University of Texas at El Paso; **YPM**, Yale-Peabody Museum, Connecticut; **ZIN**, Zoological Institute, Russian Academy of Sciences, St. Petersburg; **ZPAL**, Palaeozoological Institute of the Polish Academy of Sciences, Warsaw.

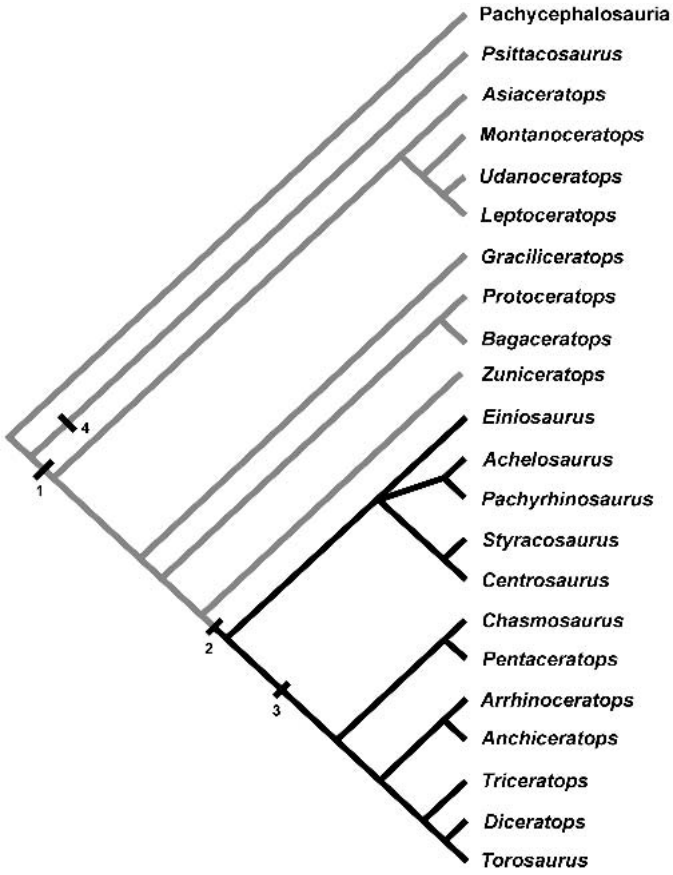

FIGURE 1. Composite cladogram of Ceratopsia created from modified versions of cladograms from Makovicky (2001: in medium gray) and Dodson et al. (in press: in black). Internode 1 refers to postcranial attributes of all neoceratopsians, internode 2 refers to postcranial attributes of ceratopsids, internode 3 refers to attributes of chasmosaurine postcrania, and internode 4 refers to attributes of *Psittacosaurus* postcranial elements. These attributes are listed in Table 1.

MATERIALS

Both isolated specimens and those from bone-beds are included in the data set. The primary data base consists of elements found in direct association with diagnostic skull material, as the taxonomy of Ceratopsia thus far has been based on skull characters. Ceratopsian anatomy is fairly well understood in terms of general descriptions, particularly in terms of comprehensive cranial anatomy studies (e.g., Hatcher et al., 1907; Lull, 1933; Brown and Schlaikjer, 1940; Maryańska and Osmólska, 1975; Sereno, 1990; Dodson and Currie, 1990; Dodson, 1996; Forster, 1996; Sampson et al., 1997). Previous postcranial studies include those of Adams (1987, 1991a, b), Lehman (1989), Tereshchenko (1991, 1994, 1996), and Johnson and Ostrom (1995), among others. The morphometric methods applied to the study of the ceratopsian postcranial elements add quantitative data to the qualitative descriptions in the literature, and allow for comparisons of specimens across both North America and Asia without the need to transport specimens.

The girdle and limb elements comprise the database for the morphometric methods used in the current study to identify trends in ceratopsian postcranial evolution (Fig. 2). The larger size of girdle and limb bones provided more complete data than were available with vertebrae, ribs, manus, and pes elements, and were also more likely to be previously identified to generic level due to associated cranial material. Accessibility of the specimens was occasionally limited because they were located behind glass or on a mounted skeleton; these could not be measured. Occasionally, it was not possible to exactly duplicate the orientation of these elements in photographs, measurements, or scale, and these elements were not included in the analyses. The total number of elements included in the analyses is 520, some from the same individual. Taxa represented include *Psittacosaurus*, nine basal neoceratopsian genera, and 12 ceratopsid genera. Several undescribed specimens were included in the analyses (i.e., TCM 2001.96.4 and MOR 300), because they are new basal neoceratopsian taxa being described, and may be compared to the other basal taxa (Chinnery, pers. obs.). Anatomical descriptions and figures as well as specimen lists can be found in the Supplemental Materials.

All measurement data were taken directly from specimens (no photographs or casts were used) and were included in the analyses. Several measurements were estimated but most were left incomplete in order to provide the most accurate data possible. Data from opposite sides of a single individual were averaged. If the measurement set for a specimen was not complete, the specimen was not included in the Principal Components Analyses (PCA—a minimum percentage of data is required for inclusion in the analyses).

Included in the shape analyses were all mostly complete and non-deformed elements. Partial elements were documented in photographs for later inclusion in the analyses. The landmarks are homologous and analogous, and were chosen to highlight element areas of interest. Missing landmarks were estimated only on nearly complete specimens in order to provide full data sets for these analyses. The Resistant-fit Theta Rho Analysis (RFTRA) and Least-Squares Theta Rho Analysis (LSTRA) in-

clude more specimens than those analyzed with Euclidean Distance Matrix Analysis (EDMA) because the latter program cannot handle extreme variability well (Richtsmeier, pers. comm.; see Methods section). In fact, most EDMA analyses not only include fewer specimens, but also compare fewer landmarks. Accordingly, some of the comparisons among the various specimens include different data sets, although variation in data sets was kept to a minimum.

The elements were carefully oriented in identical positions for measuring and photographing, so that the results were comparable. Please see the Supplemental Materials for discussion of the various orientations used and Fig. 2 for diagrams of the measurements taken and landmarks digitized.

Potential for error in a study such as this is high, and the possible sources numerous. In order to decrease this potential, only mostly to completely undistorted elements were included. Even so, some distortion is inevitable with a data set of this size, and is most likely responsible for the numerous outliers in the PCAs. Some outliers have already been eliminated from the final analyses, while others have been inspected and judged to show variation rather than deformation. Further analyses will help to decipher the remainder of the outliers. All measurements were taken with the elements at identical orientations, usually with one area held in a horizontal position (based on a liquid leveler). Photographs were likewise taken by leveled camera equipment and from identical orientations (warping of images due to shape of camera lenses is equal throughout the analyses and therefore does not affect the results), and biological landmarks were chosen based on an error study conducted prior to this project as well as previous studies (Chapman and Brett-Surman, 1990; Weishampel and Chapman, 1990). Most landmarks chosen are analogous, including extreme points and inflection points, because postcranial elements lack numerous homologous landmarks. Results of the shape analyses were analyzed with the choice of data taken into account.

METHODS

For vertebrates in general, morphometric methods have been used to understand variation in postcranial skeletal anatomy (e.g., Dodson, 1975a, 1980; Oxnard, 1978, 1983, 1984; Dawson, 1994; Van Valkenburgh, 1987; Weishampel and Chapman, 1990; Chapman and Brett-Surman, 1990; Watabe and Nakaya, 1991). However, in Neoceratopsia, these approaches have focused almost entirely on skull material (Gray, 1946; Lull and Gray, 1949; Dodson, 1976, 1990, 1993; Forster, 1990, 1996; Chapman, 1990), in large part because much of the taxonomy of this group is skull-based. Exceptions to this overwhelming emphasis on skulls are works by Lehman (1989, 1990), which focused on variation within one ceratopsid genus (*Chasmosaurus*), and Chinnery and Chapman (1998), in which a select group of ceratopsid limb elements was compared using several morphometric methods.

Linear Measurement Data Collection and Analysis

Because bone adapts to stress through life and through evolution by changing shape, changes can include increasing or decreasing length, different size or shape of crests and articular areas, and different distributions of cortical bone tissue. Many of these changes can be captured with linear measurements, and analyzed using bivariate and multivariate analyses. Some of the earlier morphometric analyses of ceratopsians were based on these methods (Brown and Schlaikjer, 1940; Gray, 1946) when data collection was relatively simple, and ratios and bivariate analyses required little computer dependence. Biometric methods, both bivariate and multivariate, have been used since then (Dodson, 1975a, 1975b, 1976, 1980; Chapman et al., 1981; Chapman et al., 1997; Chinnery and Chapman, 1998) because they are useful in allometric studies of growth, evolutionary change, and sexual dimorphism. Bivariate analyses supply information comparing two measurements, and multivariate approaches including Principal Components Analysis (PCA) combine all variables into a single analysis.

PCA is a multivariate approach used to determine similarities and differences in forms in addition to the variation most often attributable to absolute size. PCA has been successfully applied to the morphometric study of trilobites (Hughes and Chapman, 1995), painted turtles (Jolicoeur and Mosimann, 1960), *Alligator* (Dodson, 1975b), prosauropod dinosaurs (Weishampel and Chapman, 1990), pachycephalosaur dinosaurs (Chapman et al., 1981), *Protoceratops* (Dodson, 1976), and ceratopsids (Forster, 1996; Chinnery and Chapman, 1998). Principal components, or directions of variation, are computed from linear correlations, set in a matrix, between variables. Thus, all measurement data of interest can be included in a single analysis. Size difference is usually contained in the first component, especially among reptiles which can be evergrowing (Jolicoeur and Mosimann, 1960; Dodson, 1975b). Other components are thought to depict shape differences or allometric trends within or among taxonomic or age groups (Jolicoeur and Mosimann, 1960; Dodson, 1975b). Raw data are typically log-transformed in order to reduce the number of residuals and amount of heteroscedasticity (as per Reyment et al., 1984) and input into a statistics package such as Systat. Options within the Systat 8 and 10 programs applied in this project were a correlation matrix (covariance provided similar results) and pairwise deletion, the latter to include as many cases as possible even with missing data. The output of a PCA includes a component loadings matrix, which describes the amount of variation contained in each component, as well as the variable loadings within each component. A highly positive or negative loading signifies that a particular variable contributed more than the others to the variance in that component. Bivariate plots of the first and second (and other) components depict clustering, if it exists, among the groups included in the analysis. As clustering along the x-axis (the first principal component) typically indicates size difference, the focus is on any clustering occurring along the y-axis that would indicate shape differences apart from size.

The more general directions of variation obtained from the PCA can be narrowed to the particular measurements causing the majority of variation in principal components through the use of bivariate analysis. Thus, bivariate analysis is a very powerful addition to PCA, because overall results can be pinpointed to specific areas of the bone for a more precise understanding of the allometric patterns at work and the biological areas that are affected. Slopes can be compared among taxa for determination of allometric changes through evolution, following Huxley's (1932) equation of allometry ($Y = bX^a$), with X as the measurement depicting overall size of the element or organism, Y as an additional measurement of a part of this element or organism that indicates the statistical relationship between X and Y, *b* as intercept on the Y axis, and *a* as the allometric coefficient (Dodson, 1975b). Slopes over 1.0 depict positive allometric trends and those under 1.0 display negative allometry. Slopes of different taxonomic groups can be compared to find evolutionary differences among them.

Linear measurements of ceratopsian elements were first subjected to PCA in order to identify those variables that controlled size and shape variation in the sample of ceratopsian postcrania. Thereafter, these important variables were regressed against overall size of the particular elements (usually element length) and Reduced Major Axis (RMA) slopes were computed for the entire data set using Microsoft Excel and plotted using the program Slidewrite. Individual slopes were tested for significant difference using the post-hoc Tukey test available in the Analysis of Covariance (ANCOVA) part of the Systat programs. This test

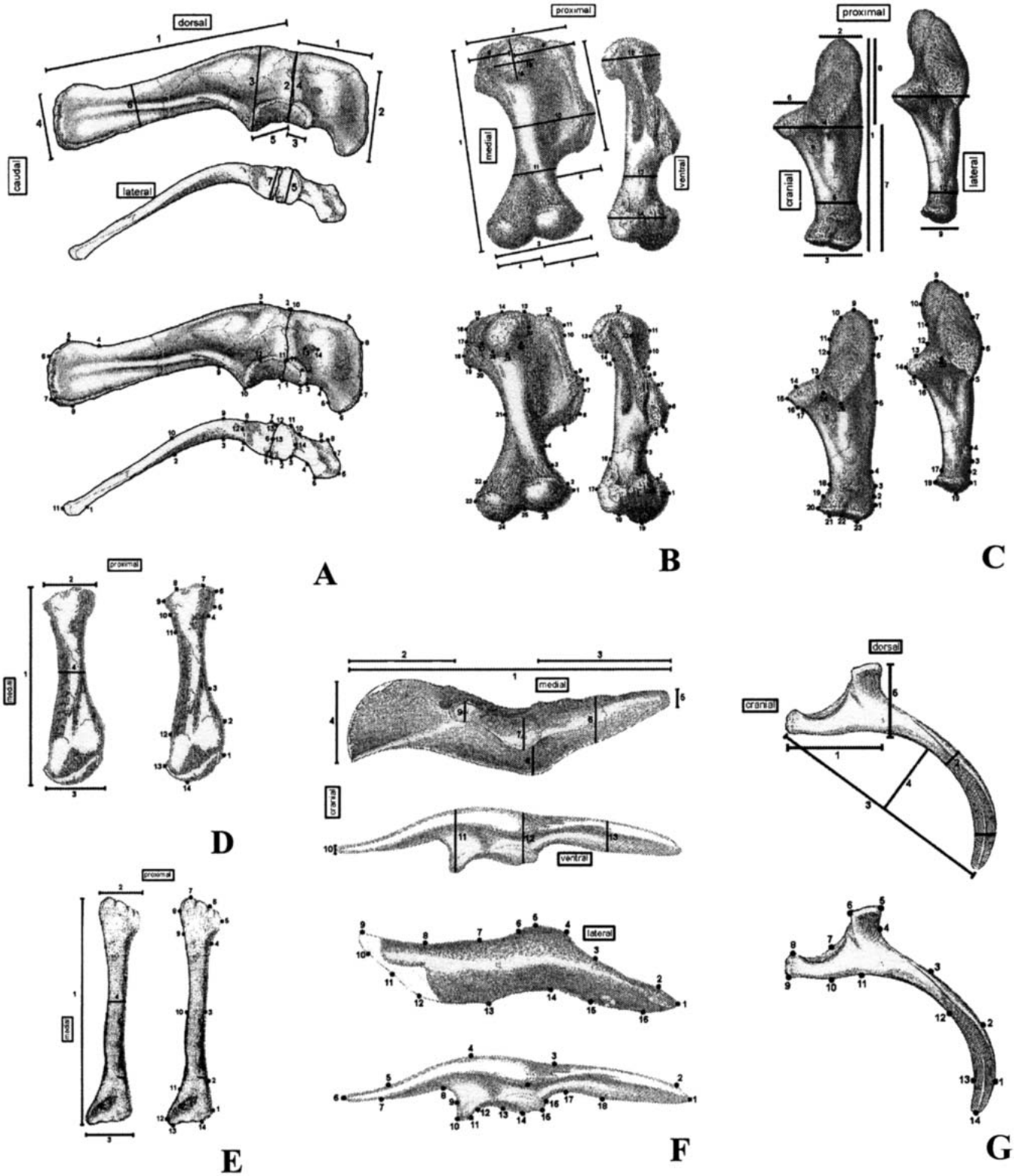

FIGURE 2. Linear measurement and biological landmark data collected on the ceratopsian material, visualized on representative elements of *Triceratops* (Hatcher et al., 1907). Measurement data are indicated by numbered lines on the top or left hand figure in each set, while landmarks are shown as numbered dots. Elements figured are: **A**, scapulocoracoid in lateral (top of each pair) and ventral views; **B**, humerus in dorsal (on the left) and lateral views; **C**, ulna in lateral (on the left in each pair) and cranial views; **D**, radius in cranial view; **E**, fibula in cranial view; **F**, ilium in ventral and lateral views for the measurement data, and dorsal and lateral views for the landmark data; **G**, ischium in lateral view; **H**, pubis in ventral (top) and lateral views; **I**, femur in cranial (on the left in both pairs) and lateral views; **J**, tibia in cranial (on the left in both pairs) and lateral view.

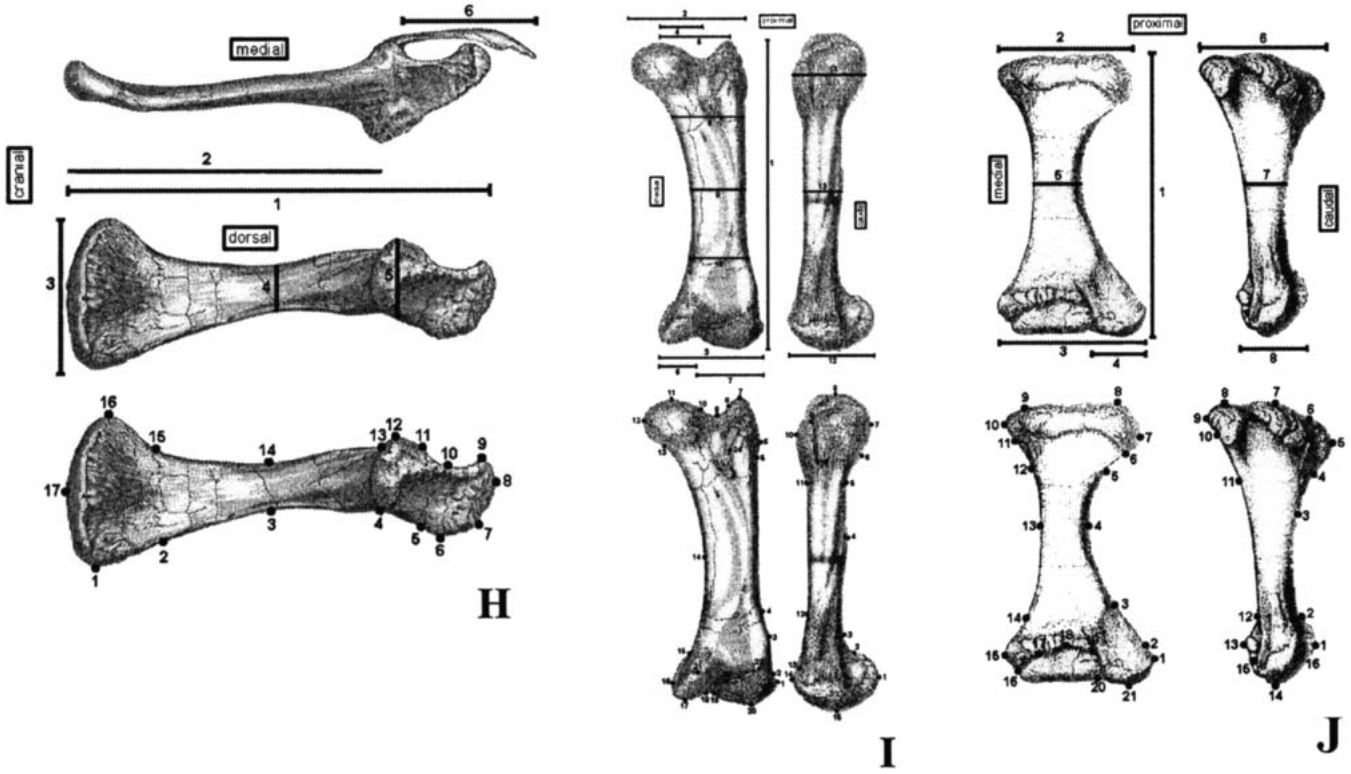

FIGURE 2. *(Continued)*

allows for and includes the error of both the X and Y variables in determination of significant statistical difference among slopes. RMA slopes are more robust than least-squares slopes, because variation on both axes is accounted for. As ceratopsian body size increased, specific areas of each element changed at different rates. The RMA slopes allow an interpretation of exactly how the individual elements changed, providing possible information on mechanical properties of the bones and changes in muscle size and use.

In a bivariate plot, clustering of individual element points may occur along different slope lines, allowing for the discussion of differing growth or evolutionary trends. Clustering along a single slope line is less dynamic, but still provides important information about the groups included.

Included with the Supplemental Materials are tables for all elements listing sample sizes, correlation coefficients, RMA values (allometric coefficients), and intercepts. Also listed are the RMA slopes that are statistically significantly different from isometry (slope = 1; $p \leq 0.05$ and 0.01), and the group slopes that are significantly different from each other ($p \leq 0.05$). Both are based not on RMA slopes, but on least-squares values, as the results are essentially equal as long as the correlation coefficient is high ($r = 0.98$ or higher; Ruff, pers. comm.). Coefficients between 0.95 and 0.98 are close enough that most differences will remain significant. Those significantly different slopes with correlation coefficients below 0.95 need to be accepted with caution, as the slopes may not differ at $p \leq 0.05$ if RMA algorithms are applied.

Biological Landmark Techniques

In addition to linear measurements, three and two-dimensional biological landmarks and the relative distances among them can provide a great deal of information on form change during ontogeny and phylogeny. Although the large size and inaccessibility of mounted elements precluded the possibility of collecting three-dimensional landmark data for this analysis, two-dimensional landmark data were obtained from images of the ceratopsian material using the program TPSDig, version 1.18 (Rohlf, 1998). These biological landmarks fall into two categories. Biologically homologous landmarks are assumed to be developmentally equivalent on all specimens (Bookstein, 1991), and include three-way cranial sutures, foramina, and other distinct and discrete points. Analogous landmarks, on the other hand, are not strictly homologous, but still provide information on similarity of shape as long as the results are interpreted in light of the data chosen. Analogous landmarks include points of inflection on element borders, extreme points (i.e., the most dorsal point of the element), and distance points (such as the midshaft point). Both homologous and analogous biological landmark data were collected for this project. Information from previous morphometric studies (including Adams, 1987; Lehman, 1989; Chapman and Brett-Surman, 1990; Chinnery and Chapman, 1998) and other sources (Romer, 1956; Dodson, 1975b) were used to determine suitable landmark sites.

Analyses were conducted using Least Squares Theta-Rho Analysis (LSTRA), Resistant-Fit Theta-Rho-Analysis (RFTRA), and Euclidean Distance Matrix Analysis (EDMA). The first two methods compare forms using superimposition, fitting one form to another, while the third method compares inter-landmark distances without the use of superimposition. The output graphics of the three methods are illustrated in Fig. 3.

Superimposition of forms is usually accomplished by using either a least-squares method as in LSTRA or the more resistant repeated means method of RFTRA (Siegel and Benson, 1982; Benson et al., 1982; Chapman, 1990; Rohlf and Slice, 1990; Chapman et al., 1997). The former uses the average distances of all points to position one form on another, thereby providing the opportunity to study form change in the entire specimen. It is

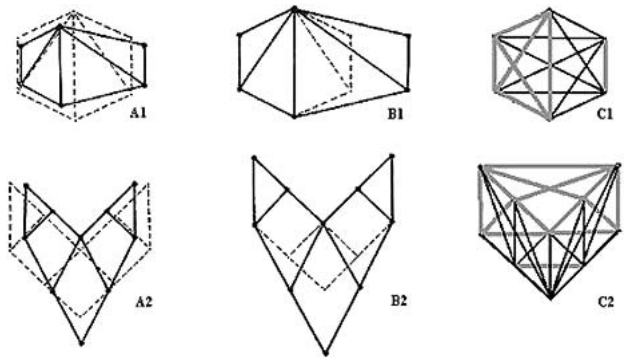

FIGURE 3. Comparison of RFTRA, LSTRA, and EDMA output graphics on a simple shape, modified from Benson et al. (1982). The EDMA graphics were produced by drawing lines between landmarks based on the Difference Matrix (DM—see text for explanation). The shapes change differently according to RFTRA (**A**) and LSTRA (**B**), and EDMA (**C**) shows only relative distance changes. Superficially, EDMA in these cases appears to resemble the LSTRA graphics. However, values in the DM can be used to determine relative magnitude of change in the interlandmark distances, and the potential errors of superimposition are avoided.

particularly applicable when the specimens being studied grow at similar rates and directions throughout the element. However, growth and evolutionary change is rarely average throughout an element, as can be seen in the bivariate plots of ceratopsian postcranial elements. By averaging the inter-landmark distances, greater change in one area is redistributed throughout the element, and potentially valuable information is lost (Siegel and Benson, 1982; Benson et al., 1982). In addition, a large change in one area of an element will "swamp out" other, more subtle changes, as the large change will be redistributed throughout the element (Fig. 3A1, A2).

Resistant-fit methods (for example, RFTRA) place the overlying form on the base form in a different manner—the most similar areas of the two forms are lined up first. The placement is made regardless of the importance of the area functionally or developmentally. This procedure allows for comparison of subtle changes that could otherwise be "swamped out" by a large deformation in one area of the shapes (Siegel and Benson, 1982) and for more precise study of localized change (Fig. 3B1, B2). Resistant-fit methods are more robust when over half of the points fit closely; if one-half or fewer points fit closely, the superimposition of the forms is arbitrary. As biological elements do not usually grow and evolve similarly throughout the element, RFTRA is probably the more accurate and valuable of the two superimposition methods in the study of ceratopsian postcrania. However, when using RFTRA one must understand that the results emphasize localized change, and may de-emphasize more important but more subtle changes in the element. With LSTRA results for comparison, though, and especially with EDMA results included as well, RFTRA results can be verified and can provide a great deal of information on element growth and evolutionary change.

EDMA uses identical landmark data, but compares forms without the use of superimposition (Lele and Richtsmeier, 1991; Lele, 1991; Richtsmeier et al., 1992; Lele and Cole, 1996). Each linear distance between two landmarks on a form is compared directly with the same distance on another form. This negates any dependence of the linear distance on surrounding distances, thus solving all of the problems associated with the superimposition aspects of LSTRA and RFTRA. Until recently, EDMA has been applied primarily to three-dimensional landmark data of skull material, and prior to this study has not been applied to postcranial material and in direct comparison with the other methods included.

The results of EDMA differ from those of LSTRA and RFTRA, and require different interpretation (Fig. 3C1, C2). In the latter two methods, both forms that are being compared are represented by the graphical output of the chosen landmarks and with vectors signifying the direction and amount of change between each pair of landmarks. EDMA provides a data matrix of the inter-landmark distances only (a Form Difference Matrix). A ratio is generated of the distance between two landmarks in the denominator (the second specimen) and the numerator (the equivalent to the base specimen of RFTRA and LSTRA in this project) for each pair of landmarks. These ratios (all are either below 1.0 [the numerator is relatively longer], equal to 1.0 [the interlandmark distance is equal], or above 1.0 [the denominator is relatively longer]) can be represented by colored lines drawn from landmark to landmark on a sample illustration. In this project, distance ratios less than 1.0 are indicated in gray, and those greater than 1.0 in black and dotted black lines, and all are drawn on illustrations of *Triceratops* elements. Black lines indicate expansion in relative size of the non-base specimen, and gray lines indicate relative contraction of distance in the non-base specimen. Directions of change are not known in EDMA as, for example, a longer interlandmark distance may be due to either or both of the landmarks moving relative to the other. However, some changes, such as rotation of a part of the element, are represented by longer inter-landmark distances in one area of the element and shorter ones in another area.

The data collected were analyzed using all of the above morphometric methods, with the goal of combining various types of output for the determination of evolutionary changes in the postcranial anatomy of ceratopsian taxa. All data were placed into one of four groups: *Psittacosaurus*, basal neoceratopsians, Centrosaurinae, or Chasmosaurinae. The basal taxa do not form a monophyletic group, but are grouped together for the purposes of determining the differences in element shape between these small taxa and the much larger ceratopsids.

Discussed here are comparisons of *Psittacosaurus* to basal neoceratopsians, basal neoceratopsians to ceratopsids, and centrosaurines to chasmosaurines, reflecting the phylogenetic context of these taxa. When more than one example of an element was available for inclusion, an average specimen was generated by each method. In effect, the average specimen of the basal neoceratopsian scapula (for example) is a composite including all basal neoceratopsian scapulae. This provides a more representative example of the element for that group, and helps to lessen the effect of preservational deformities. Use of average forms is necessary when doing form comparisons, as using each separate specimen would take an exorbitant amount of calculation time, and the selection of a single representative can provide biased results. Admittedly, averaging basal neoceratopsians is awkward due to paraphyly of the taxa, but the purpose of this part of the project was to study general trends in postcranial anatomy due to evolution (at least some of the basal neoceratopsians lived prior to the ceratopsid dispersal [Chinnery and Weishampel, 1998] and in general they exhibit a suite of more basal characters), size change (most of the basal forms are much smaller than the ceratopsids), and function (many of the basal forms have similar anatomical characteristics).

Generic-level comparisons were also made for each element, and all landmark methods were applied to these as well. Due to length constraints, these results are not included in the current paper, but can be found in the Supplementary Materials. Generally, these individual comparisons were conducted for one of several purposes. Enigmatic taxa, including *Graciliceratops*, *Avaceratops*, and *Brachyceratops*, were compared with others to determine how close in shape the elements are to those of (supposed) closely related taxa. Basal neoceratopsian genera from

the same continent (either Asia or North America) or from each continent were compared for the purpose of seeing how close the relationships or functional attributes are between the two continents. Finally, members within Centrosaurinae and Chasmosaurinae were compared to see if postcranial attributes could be found at the generic level in these two subfamilies.

The results are of a qualitative nature, whereas the methods used are all quantitative in nature. Results from all five methods employed were compared prior to the final interpretations, and consequently many of the evolutionary and functional trends discussed here are qualitative in nature. Output parameters of the shape analyses (difference coefficients in RFTRA and LSTRA and a distance ratio number in EDMA) provide the quantitative output for these methods, and can be found with the Supplemental Material. These parameters were combined with results of the multivariate and bivariate analyses, prior information of element differences, and knowledge of functional areas of the elements. For example, LSTRA may superimpose a specimen differently onto a base specimen than does RFTRA due to the averaging of the landmark distances. RFTRA lines up the landmarks with the least amount of apparent change first, but the superimposition can still be faulty. EDMA graphics tell which distances are longer and shorter, but not which landmarks have changed position to cause the distance changes. The combination of all results is necessary to gain the most accurate conclusions, and therefore the discussions are more qualitative than quantitative.

RESULTS AND DISCUSSION

Evolutionary Patterns

Evolutionary patterns among ceratopsian dinosaurs can be indicated in several ways. Bivariate plots of the components in a PCA show clustering if the groups are different in shape. The four groups included in this project, *Psittacosaurus*, basal neoceratopsians, centrosaurines, and chasmosaurines, are by default already clustered in each graph due to size (indicated in Component 1, the x-axis variable [C1]). No *Psittacosaurus* or basal neoceratopsian elements are as large as those of the adult ceratopsids. The y-axis in a C1/C2 or C1/C3 plot is the axis of interest, and any clustering along this axis indicates form differences and possibly phylogenetic differences. If the only distinct clustering is seen along the x-axis, the conclusion is that the element increases in shape solely in response to size increase.

The RMA slopes in the bivariate plots depict general evolutionary trends. RMA slopes above 1.0 indicate that the y-variable increased in size at a greater rate than the generalized 'size' variable (usually length of the element), and slopes below 1.0 indicate the opposite. Although *Psittacosaurus* is the outgroup to Neoceratopsia, in the majority of measurements all data points are located close to the RMA line, suggesting much similarity in the postcranial elements within Ceratopsia. This similarity is forced, in part, by the inclusion of all specimens in the regression equations. However, relative positions of the groups around the regression line can still be compared. Different slopes for each group in the analyses show allometric patterns—as size increases, traits change at different rates. Not many group slopes differ from each other at a statistically significant level, and therefore the ones that do differ are important for phylogenetic distinction.

General Evolutionary Trends Throughout Ceratopsia

The groups included in the analyses cluster differently in the various PCA bivariate plots of C1 and C2. The first component of nearly all analyses contains a very large percentage of the variance, verifying that size is the primary change within Ceratopsia in these elements. Subsequent components contain such small percentages of the variance that the following interpretations must be viewed with caution. However, size change through evolution is understood in this clade; we are interested in other shape changes, and therefore the small differences are important. *Psittacosaurus* elements generally cluster together (it is only one genus, while the other groups contain more than one genus, so this clustering is expected), and the more derived condition of some of the elements is apparent in the clustering of these small elements along C2 with the much larger chasmosaurine elements, especially in the scapula, coracoid, femur, and tibia (Figs. 3A, 3B, and 3C). Closer relationships in these analyses to the basal neoceratopsians might be expected if the neoceratopsian common ancestor was psittacosaur-like, and especially considering the greater similarity in size of the elements in psittacosaurs and basal neoceratopsians compared with those of the ceratopsids. From these analyses it appears, however, that evolution within Psittacosauridae along with element differences due to functional changes (see Functional Morphology section) have reduced similarities in many postcranial elements with those of basal neoceratopsians.

Basal neoceratopsians plot similarly to centrosaurines along the C2 axis in the ilium (first PCA), ischium (Fig. 4G), and tibia (second PCA), and are located with the chasmosaurines in the radius (first PCA; Fig. 4F), femur (first PCA; Fig. 4B), tibia (first PCA; Fig. 4C), and fibula. Basal neoceratopsians cluster less than the other groups reflecting the paraphyly of the group, especially in the scapula (Fig. 4A), coracoid, humerus, and femur. However, all plot apart from the ceratopsids in the radius (second PCA; Fig. 4D), ilium (Fig. 4I), and pubis (Fig. 4E). This mixture of relationships shows the more basal nature of the basal neoceratopsians, and that various areas of various elements evolved differently, some remaining similar to the basal neoceratopsian condition and others changing to a greater degree.

Centrosaurines routinely cluster apart from chasmosaurines in the PCA plots. In the scapula (first PCA; Fig. 4A), coracoid, radius (first PCA; Fig. 4F), ischium (Fig. 4G), pubis (Fig. 4E), and tibia (Fig. 4C), the centrosaurines cluster primarily on the positive side of the C2 axis, while the chasmosaurines are typically located on the negative side (apart from outliers). Overlap on the C2 axis of these two groups occurs in some of these (coracoid and tibia), but the rest are more discrete clusters. Divisions at the subfamily level are still apparent but positions are reversed in the second scapula PCA as well as the radius, ilium, and fibula plots, in which the centrosaurines are primarily located below the zero axis of C2 and chasmosaurines above. Thus, these two monophyletic groups quite definitely exhibit postcranial differences at the subfamily level. The variables contributing to the location of these taxa along C2 seem fairly arbitrary as far as the above groupings are concerned (no similarity of variables occurs in the clustering of centrosaurines positively in specific elements and negatively in others).

Taxonomic variation within the subfamilies of Ceratopsidae can be found in the humerus, in which two distinct groups are apparent in each subfamily on the C2 axis of the first PCA (greater dorsoventral width of the shaft on the positive side of the zero axis and wider lateral side of the proximal end below the axis; Fig. 4H), and in the second humerus PCA in which both groups are spread across C2. Centrosaurines also do not cluster in the tibia PCA, suggesting interspecific variation in this element (the main contributing variables being the proximal width and the calcaneal facet width; Fig. 4C). Although division of the subfamilies is most likely due to intrataxonomic variation even when genera are themselves divided, sexual dimorphism is a plausible alternative hypothesis to be considered. Further analyses will help to resolve this issue.

Within Centrosaurinae, *Pachyrhinosaurus* elements cluster together in the coracoid PCA (with large glenoid fossae), and *Centrosaurus* humeri cluster along with *Styracosaurus* ones (with

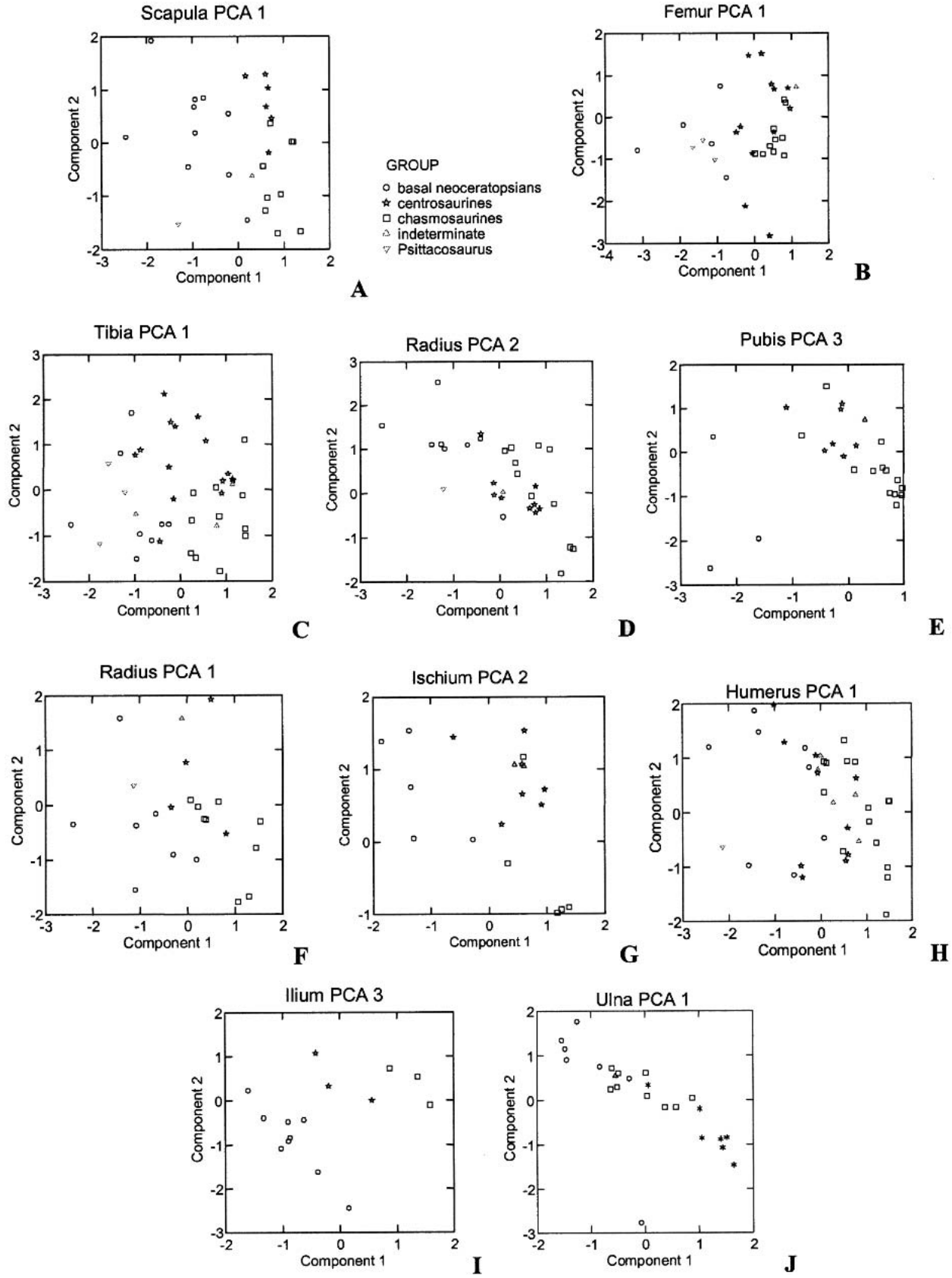

FIGURE 4. Selected bivariate plots of the first and second components of Principal Components Analyses (PCA) of ceratopsian postcranial elements. Component loadings tables are available with the Supplemental Materials (Appendix).

wide dorsoventral shafts). *Centrosaurus* and *Styracosaurus* humeri are separated from those of *Einiosaurus*, *Monoclonius*, *Pachyrhinosaurus*, and *Avaceratops* (heads positioned more medially). Therefore, this analysis supports the close relationship of *Centrosaurus* and *Styracosaurus* (Fig. 1) but does not support the possibility of the *Monoclonius* material as juvenile *Centrosaurus* (although this does not preclude the nomen dubium material from belonging to other centrosaurine taxa; Sampson et al., 1997).

Several PCA analyses appear to show negative correlations between C1 and C2, including the radius (second PCA; Fig. 4D) the pubis (through ceratopsids only; Fig. 4E), and the sinuous pattern seen in the ulna (Fig. 4J). These plots show clear patterns of change in the elements as size increases. In the radius, as size increases the mediolateral width of the proximal end increases at a relatively higher rate (length is decreasing relative to the breadth of the proximal end as size increases). In the pubis, the articular area becomes taller in the larger elements (relative length of the element decreases with size). In the ulna, the rates of decrease are higher among the smaller-sized individuals of each group. As the specimens become larger in size, the rate lessens and then increases again with the largest individuals. Although a hypothesis of size as the primary influence on the C2 values is possible, evolutionary mechanisms are most likely partially responsible due to a difference in the pattern formed by the growth analysis (Chinnery, pers. obs.). According to the maximum loadings in the analyses as well as the bivariate plots, the C2 values are primarily the relative lengths of the proximal and distal portions of the ulna. As the individuals become larger, the distal length decreases relative to the proximal length, at first abruptly and then at a slower rate before decreasing at a higher rate again. Functionally, this means that the triceps in-lever is increasing and the out-lever decreasing, therefore increasing the power of the muscle.

The scapula RMA slopes show a greater increase in mediolateral width than in height of the element as length increased, with a slope of 1.209 versus the lowest height slope of 1.04 (highest height slope is 1.192; Figs. 4A1, A2). This pattern shows a greater relationship between increasing structural support (weight bearing) and increasing size, rather than increasing surface area for muscle attachments. Slopes are significantly different from isometry except for the articular area height and the maximum height of the scapula, both at the proximal end of the element. Thus, the more distal part of the element (and the lateral width) increased more through evolution.

Coracoid glenoid fossa length increases more with maximum coracoid length than do the other measurements. Only this measurement and maximum width of the element differ from isometry (at the $p \leq .01$ level). The groups are not significantly different from each other in any measurement, suggesting very similar allometric trends among them.

As humeral length increases, mediolateral widths increase with positive allometry; 1.215 proximally, and 1.238 distally. As the deltopectoral length increases at a low slope with length of the element among these taxa (slope = 1.09), the distal portion extends farther laterally with length (slope = 1.403; Figs. 4B1, B2). The relationship of the humeral head to the proximal end of the element changes with length, as the proximolateral corner grows more than the proximomedial one. The remaining areas of the element tend to increase with slopes ranging from 1.2 to 1.3. All slopes are significantly different from isometry, even the deltopectoral crest length slope of 1.09, the latter due to the correlation and intercept values. Significant differences between the group slopes occur in nearly all mediolateral width measurements, the exceptions being the distance from the head to the medial border of the element and minimum shaft width. In almost all graphs, the slopes for the *Psittacosaurus* elements are lowest, and those for Chasmosaurinae are highest. The low regression slope of the deltopectoral crest length does not accurately reflect change in this feature, as the scatter pattern is curvilinear, concave to the slope line and reflecting the large crest lengths of *Psittacosaurus*, the relatively smaller crests of the basal neoceratopsians, and then the increase in crest size with length of the ceratopsid elements (Fig. 5B1).

Proximal width of the ulna increases at a higher rate than distal width, and maximum width of the element across the sigmoid fossa rim increases at a rate greater than those of the remaining measurements (a result of a necessary increase in strength of the articulation with the humerus as the animals became larger). All regression slopes differ significantly from isometry except for the length of the proximal and distal parts of the ulna, and none of the group slopes vary significantly. The slope pattern is again one of the chasmosaurines having higher slopes than the other taxa, with one exception. Length of the ulna from the olecranon rim to the distal end of the bone is lowest in chasmosaurines, higher in basal neoceratopsians, and highest in centrosaurines (Figs. 4C1, C2).

The size, or robusticity, of the radius increased much more through the evolution of this group than the other forelimb elements, with regression slopes between 1.285 (craniocaudal shaft width) and 1.51 (mediolateral distal width), and all vary significantly from isometry. Chasmosaurine slopes are again higher than those of the centrosaurines and the basal neoceratopsians.

The ceratopsian pelvic girdle shows the most distinct evolutionary changes of the postcranial skeleton, especially in terms of the eversion of the dorsal ilium, the increasing curvature of the ischium, and the expansion of the prepubis in ceratopsids. Although these patterns in the pelvic element analyses are apparent, the mechanisms are less clear. Pelvic elements were rare for the growth analyses, and therefore some possibly important information is lost from the evolutionary analyses. Ilium widths increase at higher slopes than length and height measurements with slopes of 1.4–1.7 versus 1.0–1.2. Ischial and pubic peduncle lengths change the least (slopes = 0.8). Length slopes are similar among the groups, but width and height measurements are characterized by the highest slopes occurring with the chasmosaurines and, in nearly all cases, the lowest slopes are exhibited by the centrosaurines. The ilium expanded mediolaterally as the length increased, most likely to provide expanded muscle attachment sites for the larger limb and tail muscles, but this expansion is more pronounced in the chasmosaurines. The intermediate position of the basal neoceratopsian slopes suggests that with length increase, width increase was just as important as in the ceratopsids. However, the small numbers of specimens included make this a tentative and preliminary observation.

The ischium changed primarily as previously mentioned, with greater curvature of the ischial shaft. As articular length increased, the length of the element (measured in a straight line) increased with the highest slope in chasmosaurines, followed by basal neoceratopsians and centrosaurines. Increase in curvature occurred with nearly identical slopes in the two ceratopsid groups, and height of the articular area increased at a slightly higher rate in basal neoceratopsians than in ceratopsids. Again, small sample sizes and also a lack of a good size variable make these conclusions very tentative.

The bivariate analyses of pubes include only two basal neoceratopsian elements, and any discussion of the slope patterns in this group are suspect. However, in all plots the longer basal neoceratopsian element is noticeably larger, suggesting that increase in dimensions apart from length occurred at a higher rate among these more basal forms (Fig. 5D).

In the bivariate plots of femora, the groups are all located on or very close to the RMA slope, suggesting little difference in the element structure among taxa. All measurements are positively allometric compared with length of the element, the mediolateral width from the head to the greater trochanter, and the width at

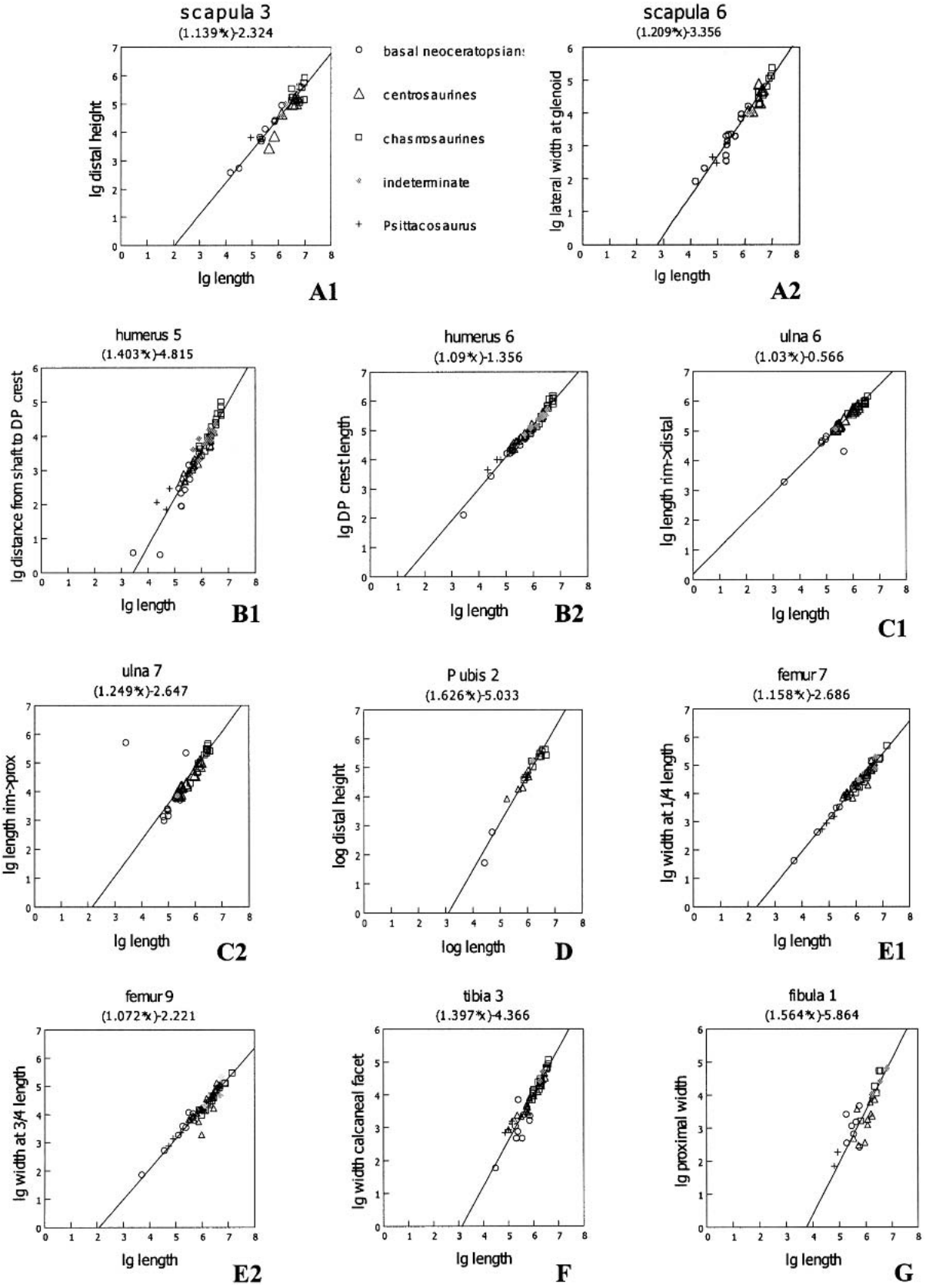

FIGURE 5. Selected bivariate plots of ceratopsian postcranial elements, including Reduced Major Axis (RMA) slope lines calculated on all specimens and RMA slope equations. See the Supplemental Materials and text for additional information on the x- and y-axis variables. Data are measured in millimeters and are log-transformed.

one-quarter length having the highest slopes, whereas width at three-quarter length and distal mediolateral width have the lowest (Figs. 4E1, E2). Thus, throughout the clade the proximal end of the element expands more as length increases than does the distal end, presumably owing to a need to increase strength at the pelvic girdle with increasing weight. With phyletic size increase, the lateral condyle increases at a greater rate than the medial condyle, suggesting a shift of the femur laterally and a longer lateral condyle for continued articulation with the tibia, or a change in knee biomechanics.

The tibia is characterized in the bivariate analyses as being similar in the ceratopsid subfamilies, but the plots indicate much more variation among basal neoceratopsians. In all, the chasmosaurine slope is the highest, followed by the slopes of the centrosaurines and *Psittacosaurus*, and finally the lower basal neoceratopsians. Again, all width measurements are positively allometric, with the highest slope indicating that the calcaneal facet expands mediolaterally more than other areas of the element with length (Fig. 5F). This suggests a strengthening of the lateral aspect of the ankle, and may correspond to the suggested shift in the femur discussed above.

The dimensions of the fibula all increase at high rates compared to length, from 1.2 up to 1.6, and more variability is evident within the groups, possibly due to preservational differences (Fig. 5G). The highly positively allometric slopes indicate that the element increased more in robustness as length increased than did other hind limb elements, a trend similar to that seen in the forelimb, where the radius exhibited the largest regression coefficients. Again, this may be due to the increase in structural support needed to support the larger animals.

Shape Differences Between *Psittacosaurus* and Basal Neoceratopsian Postcrania

The following observations are again drawn on a combination of all three shape analyses applied. Not all figures could be included, but they are available with the Supplementary Materials.

The basal neoceratopsian scapula is shorter both proximally (owing to its smaller acromion process) and distally (reflecting expansion of the scapular blade in *Psittacosaurus* [Fig. 6A1–A4]). This group of figures demonstrates the graphical output of the various shape analyses. The distal expansion of the *Psittacosaurus* scapula seems to be concentrated at the ventral corner, causing the distal end to appear shifted dorsally as compared with the proximal end. The RFTRA output shows this trend especially well. Both the scapular and coracoid contributions to the glenoid fossa are smaller in basal neoceratopsians than in *Psittacosaurus*, and the humeral head is also larger in *Psittacosaurus*. The *Psittacosaurus* coracoid is very diagnostic, resembling the neoceratopsian coracoid only in lateral view (Fig. 6C1, C2). In ventral view, the prominent division of the *Psittacosaurus* distal coracoid is clear, separated by a deep groove. The basal neoceratopsian humerus is less robust than that of *Psittacosaurus*, with a smaller deltopectoral crest and a narrower head (Fig. 6E). No *Psittacosaurus* ulnae were available for inclusion in this analysis. The basal neoceratopsian radius is more rounded both proximally and distally than in *Psittacosaurus*, and the most distal point is located more laterally.

The basal neoceratopsian ilium is taller than that of *Psittacosaurus*, and both the pubic and ischiadic processes are larger (Fig. 6K). The iliac contribution to the acetabulum is greatest compared to length in the basal neoceratopsian element. This is also the case with the ischium; the pubic and iliac peduncles of the *Psittacosaurus* ischium are close enough to each other to suggest little or no contribution of the element to the acetabulum.

Contrary to the expected reduction of the femoral head owing to the acetabular differences noted above, the femoral head of *Psittacosaurus* is only slightly smaller in relative size than those of basal neoceratopsians (Fig. 6P). The distal end of the basal neoceratopsian femur as well as the shaft is less robust, the distal articular areas are smaller, and the greater trochanter is better developed than those of *Psittacosaurus*. This last observation is notable in light of the much smaller mediolateral proximal tibia in *Psittacosaurus*. The proximal tibia is instead more expanded in this group in a craniocaudal direction than in basal neoceratopsians, suggesting a difference in orientation of the femur-tibia articulation (Fig. 6R). Distally, the basal neoceratopsian tibia is less robust than that of *Psittacosaurus*, and the astragalar facet is larger in both height and width. The same trends occur in the fibula of the two groups.

Postcranially, *Psittacosaurus* differs more from basal neoceratopsians than from ceratopsids, and the differences discussed above suggest a combination of plesiomorphic and apomorphic characters in the *Psittacosaurus* postcrania. Some plesiomorphic (ancestral) characters are found in the forelimb and pelvis, and may be associated with bipedality. Apomorphic (derived) characters include the greater robustness of all of the *Psittacosaurus* elements.

Shape Differences Between Basal Neoceratopsian and Ceratopsid Postcrania

The increase in robustness of the ceratopsid shoulder girdle is exhibited by a larger articular area of the scapula and coracoid (Fig. 6B1, B2). This articulation is wider in ceratopsids in ventral view, thus mediolaterally strengthening the narrower dimensions of the elements. In particular, the medial side of the glenoid fossa articulation is expanded in the ceratopsid scapulocoracoid.

Other examples of increased robustness of the ceratopsid shoulder girdle include a more caudal position of the ventral curvature of the dorsal border of the scapula in ceratopsids (Fig. 6B1). In ceratopsids, the distal scapular blade is taller and shifted more ventrally than in basal neoceratopsians, the glenoid fossa is increased in size, and less mediolateral curvature is evident throughout the scapula. The coracoid body is shifted from a squared shape with a large craniomedial corner in basal forms to a wider, shorter shape in ceratopsids with a longer caudal projection (coracoid process).

The basal neoceratopsian scapulocoracoid is more mediolaterally curved than that of ceratopsids, indicative possibly of a difference in position of the element on the rib cage or of a difference in curvature of the rib cage. A caudal shift of the scapulocoracoid would help to support a more horizontally positioned humerus (discussed below), as well as possibly increasing the stability in the front of the body and in the support of larger skulls in ceratopsids. Skulls and frills of basal neoceratopsians are relatively smaller than the more elaborate and developed ceratopsid skulls, and musculature extending from the scapula to the back of the skull (mm. trapezius and levator scapulae) may have been more developed in the latter. Certainly, the overall mass of the body that the forelimbs needed to support was higher in ceratopsids. Position of the element may have differed through either a shift of the element caudally and/or dorsally in ceratopsids, which would position it over more of the rib cage, and is suggested by a flattening of the rib cage seen in some specimens. The shift in position of the scapulocoracoid may also be explained by an increase in the thorax dimensions in ceratopsids due to relatively larger heart and lungs in these larger quadrupeds (Sampson, pers. comm.).

The humeral head is positioned more medially in ceratopsids, and the distal humerus is shifted slightly in a ventral direction (Fig. 6F). The deltopectoral crest of the ceratopsid humerus is larger, longer, and extends farther laterally. The olecranon process of the ulna is longer in ceratopsids than in basal neoceratopsians, and the caudodistal corner is more pronounced (Fig.

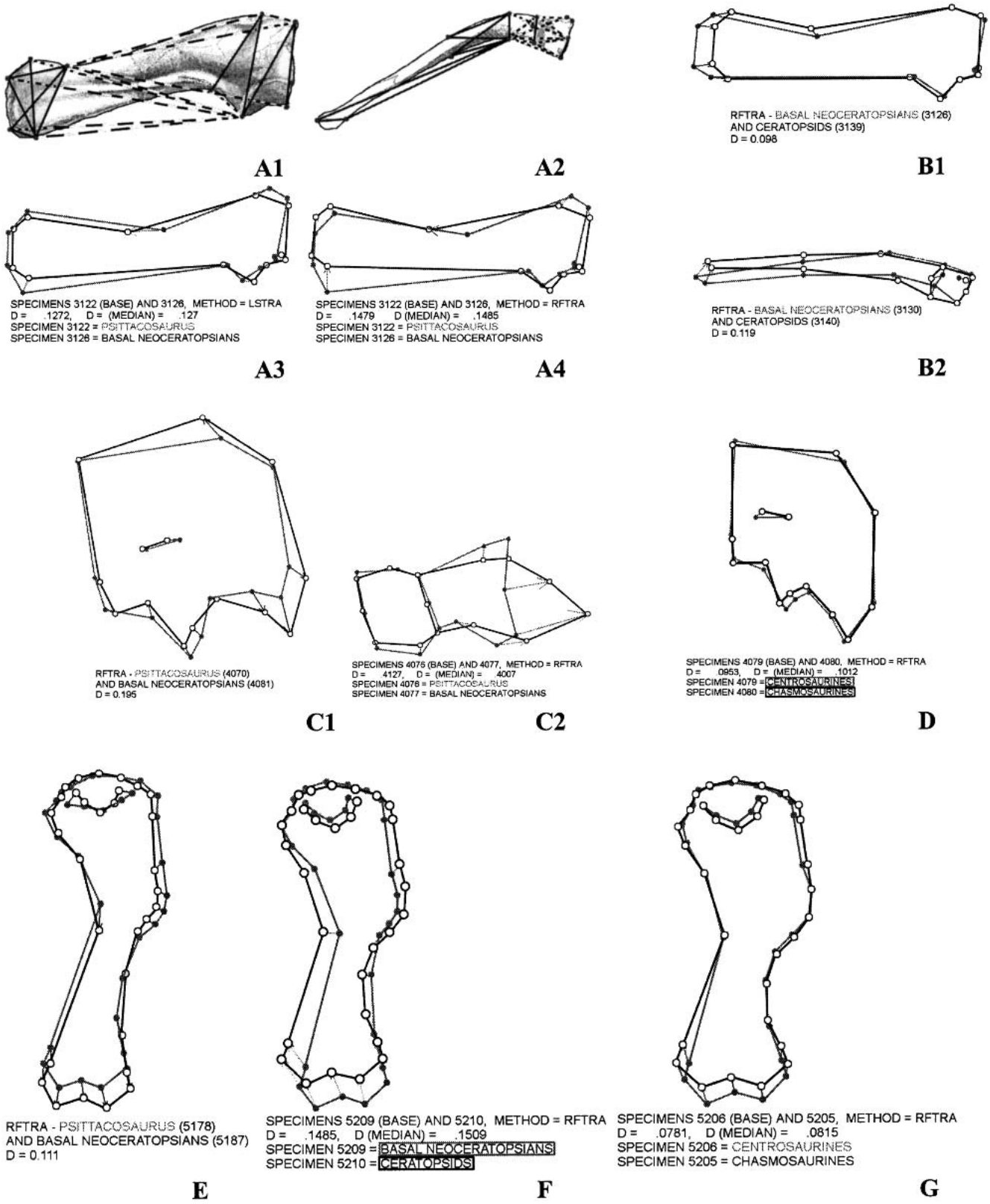

FIGURE 6. Selected shape comparisons of ceratopsian postcranial elements. The element analyses are shown in the following order: scapula (**A1**, **A3**, **A4**, **B1** in lateral position; **A2**, **B2** ventral), coracoid (**C1**, **D** [lateral], **C2** [ventral]), humerus (**E**, **F**, **G** [all dorsal view]), ulna (**H1-2** [lateral view]), radius (**I**, **J** [cranial view]), ilium (**K**, **L**, **M1** [lateral view], **M2** [dorsal view]), ischium (**N**, lateral view), pubis (**O1-3** [lateral view]), femur (**P**, **Q** [cranial view]), tibia (**R**, **S**, **T** [cranial view]), and fibula (**U**, cranial view). Resistant-Fit Theta-Rho Analysis (RFTRA) and Least-Squares Theta-Rho Analysis (LSTRA) analyses are labeled, and Euclidean Distance Matrix Analyses (EDMA) are indicated by gray and dotted black lines on illustrations of *Triceratops* elements modified from Hatcher et al., 1907. Please see the Methods section for additional information.

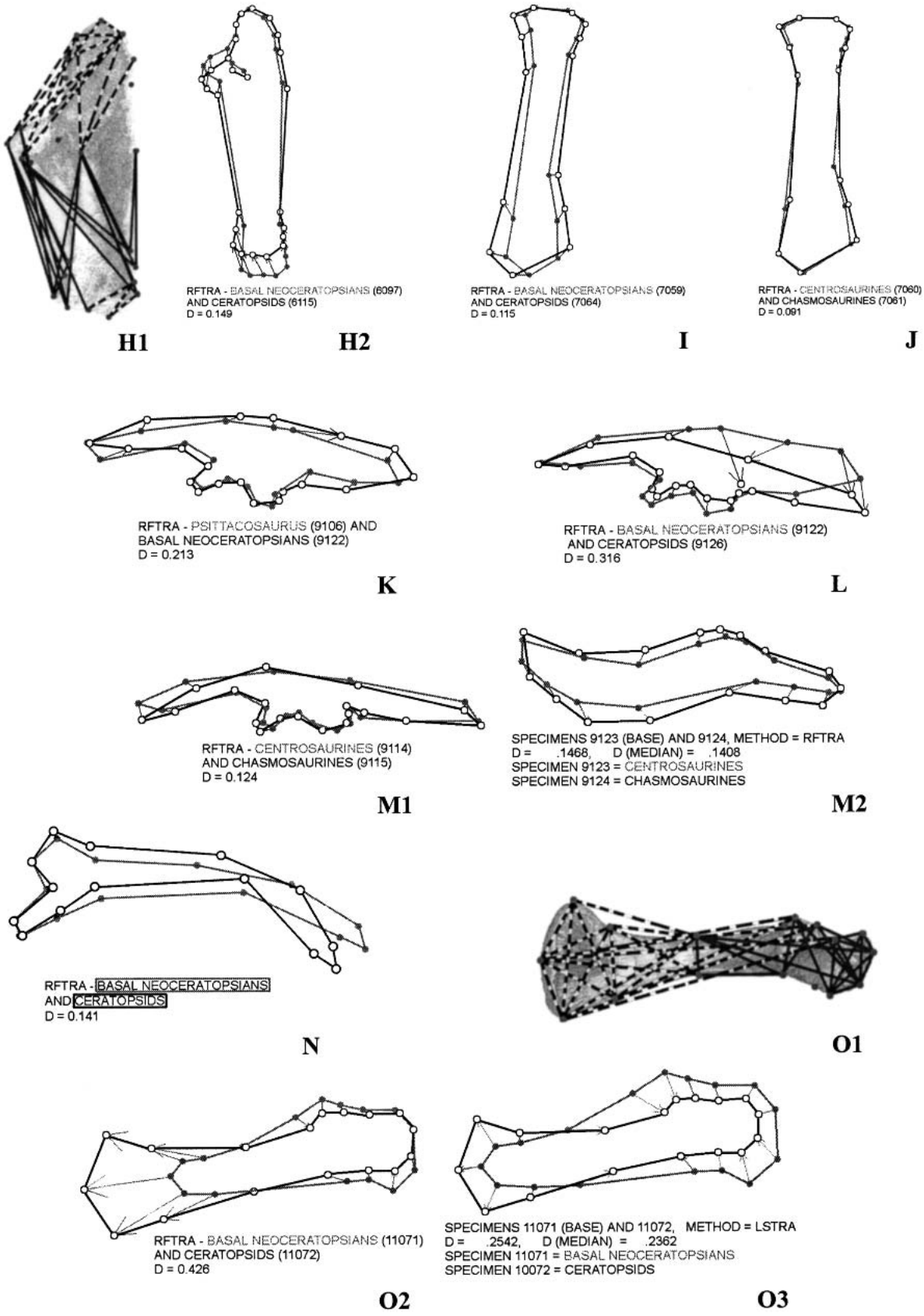

FIGURE 6. *(Continued)*

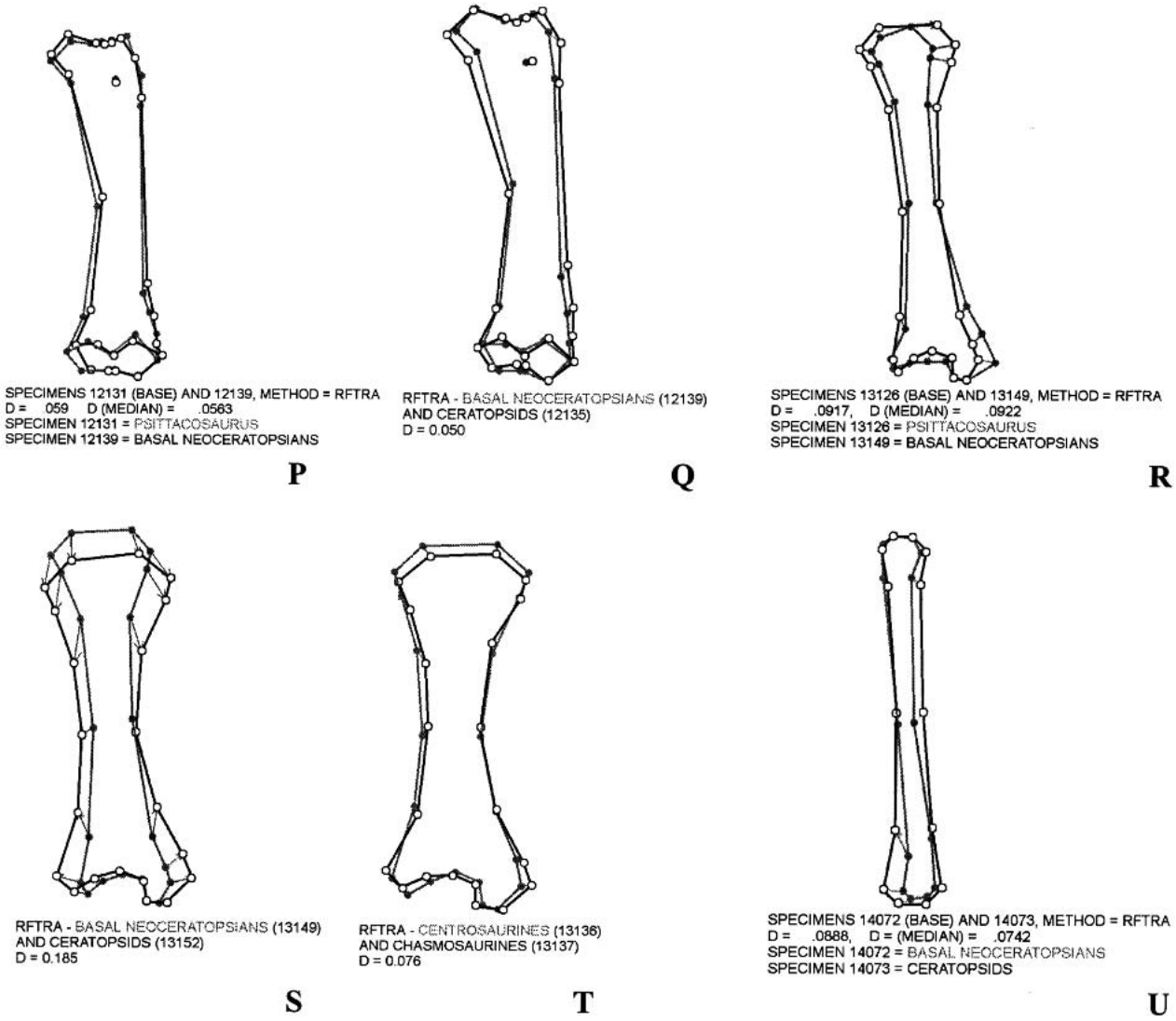

FIGURE 6. *(Continued)*

6H1, H2). In the ceratopsid radius, the proximomedial corner is more expanded than the proximolateral corner compared to those of basal neoceratopsians, and the most distal point of the distal end of the element is located more medially (Fig. 6I).

The pelvic girdle of the ceratopsid skeleton is both more robust and different in shape from that of basal neoceratopsians. Function of the hind limb does not appear to have differed much between the two groups, as the hind limb elements and the dorsal and caudal vertebrae are very similar. The girdle elements are expanded in order to accommodate the greater musculature needed to support the more massive body of the ceratopsids.

The major change in the ilium is the lateral eversion of the iliac blade in ceratopsids (Fig. 6L). Thus, the height of the element is greater in basal neoceratopsians, and the mediolateral width is greater in ceratopsids. The pubic peduncle is shorter in ceratopsids, suggesting a decrease in the iliac contribution to the acetabulum. However, in the basal forms the ischium and pubis are both taller through the area of articulation with the pubic peduncle than in ceratopsids, and so a relatively smaller bony acetabulum is present in the ceratopsid pelvis.

The ischial shaft is more curved in ceratopsids than in basal neoceratopsians (see Adams, 1987 for one explanation of the increased curvature; Fig. 6N). The pubic peduncle is longer than that of the basal neoceratopsian ischium, in contrast to the iliac peduncle, and the consequence is a caudodorsal rotation of the element and greater articulation between the ischium and the pubis in ceratopsids. The rotation is an alternate explanation for the increase in curvature of the shaft, or is a response to the curvature.

The pubis changes dramatically from the basal forms to the ceratopsids, as the prepubic process is greatly expanded both in length and in height (distal expansion), accompanied by a corresponding decrease in size of the pubic body (Fig. 6O1–O3). The larger articulation of the ceratopsid ischium and pubis discussed above could explain the decrease in size of the pubic body, as the extension of the pubic body down the ischial shaft of basal neoceratopsians may have provided additional support to the articulation of the elements.

As with the rest of the postcranial skeleton, the hind limb elements increase in robustness through this part of the phylogeny. The changes are more conservative than those observed in the fore limb, as the hind limb is columnar and the stance is similar among basal neoceratopsians and ceratopsids. Bipedalism has been suggested for basal neoceratopsian taxa by some authors (mainly *Graciliceratops* [Maryańska and Osmólska, 1975; Sereno, 2000] and *Archaeoceratops* [Dong and Azuma,

1997]) based primarily on limb ratios and immature specimens (Maryańska and Osmólska, 1975; Sereno, 2000). The forelimb and pelvic differences found in *Psittacosaurus* have not yet been confirmed in any basal neoceratopsian taxon. As with the radius, the greatest increases in robustness of the hind limb are seen in the smallest element, the fibula.

Femoral differences due to the increase in robusticity include an increase in the height of the greater trochanter and an extension of the cranial trochanter laterally, both owing to increases in moment arms acting around the hip joint (Fig. 6Q). EDMA shows that the ceratopsid femoral head is taller than those of basal neoceratopsians. Because the bony acetabulum is relatively smaller in ceratopsids (see section on pelvis), the femur either fits more tightly into the bony acetabulum in ceratopsids (e.g., the joint capsule is tighter), or it articulates obliquely relative to the vertical plane. The latter condition would cause a lateral shift of the distal end of the femur. As the distal condyles do not seem to differ between the two groups aside from robusticity, the former is the more parsimonious interpretation.

Increase in robustness of the tibia is concentrated on the medial side of the element, according to both RFTRA and LSTRA results (Fig. 6S). Distally, the astragalar facet is similar in width in the two groups, but the medial side of the facet is taller in ceratopsids. Greater width of the ceratopsid calcaneal facet indicates an increase in weight bearing of the lateral aspect of the ankle. The only shape difference in the fibula apart from the overall increase in robustness is a slight shift of the distal end of the element medially in ceratopsids (Fig. 6U).

Shape Differences Between Chasmosaurine and Centrosaurine Postcrania

The chasmosaurine scapula is characterized by greater robustness than the centrosaurine element, with the distal end extending farther dorsally than in the latter subfamily, and the proximal end extending farther ventrally due to the larger glenoid fossa rim. The coracoid contribution to the glenoid fossa is, in contrast, larger in the centrosaurine element (Fig. 6D).

The humerus, radius, and ulna are also more robust in the chasmosaurine skeleton, whereas length measurements are relatively longer in the centrosaurine elements (Fig. 6G, J). In the ulna, the distance from the sigmoid fossa rim proximally is longer in chasmosaurines, and the distance from the rim distally is longer among centrosaurines.

Shape differences between the pelves of the two subfamilies include greater dorsal and ventral curvature of the iliac blades, as well as a larger acetabulum contribution and greater mediolateral width of the chasmosaurine ilium (Fig. 6M1, M2). The chasmosaurine ischium is more curved than that of centrosaurines, an observation made previously by several authors (Adams, 1987; Dodson and Currie, 1990). The pubis is also more robust in chasmosaurines, with a more vertically extended distal end and longer articular area.

The chasmosaurine femoral head is taller than that of centrosaurines, the medial condyle extends farther distally, and the cranial trochanter diverges from the shaft farther distally (Fig. 6R). The proximal end of the tibia is larger in centrosaurines in lateral view, and larger craniocaudally in chasmosaurines (Fig. 6T). The distal end of the chasmosaurine tibia is also wider mediolaterally. Finally, the fibula is wider distally among chasmosaurines.

Phylogenetic Positions of Postcranial Differences in Ceratopsia

The changes in the postcranial skeleton discussed above were applied to a composite cladogram for the purpose of determining if and how the postcranial characters will support current cladistic analyses. The cladograms of Makovicky (2002) focusing on basal neoceratopsians and Dodson et al. (in press) with the focus on Ceratopsidae are the most current and comprehensive analyses available at this time. The composite cladogram (Fig. 1) is simply the addition of one to the other; no nodes are displaced.

Characters supporting Neoceratopsia, Ceratopsidae, and Chasmosaurinae are listed in Table 1 for all elements (when available). *Psittacosaurus* elements were compared with those of pachycephalosaurs in an attempt to determine if derived states of characters exist (Maryańska and Osmólska, 1974; Maryańska, 1990). Characters at the generic level were also inserted into the composite cladogram for each element (see Appendix). As the shape changes are comparisons of only two (usually composite) groups at a time, only those that include taxonomic groups included in the composite cladogram are included. Comparisons of taxa not recognized by Makovicky (2001: TCM 2001.96.4) and Dodson et al. (in press: *Monoclonius*, *Brachyceratops*, and *Avaceratops*) were not included. Thus basal neoceratopsians and genera within the ceratopsid subfamilies were variously compared, depending on the specimens available.

The results listed in Table 1 and discussed throughout this paper are qualitative in nature due to the combination and comparison of the five quantitative methods employed. The quantitative results individually are not necessarily accurate representations of phylogenetic differences, and should be applied with caution. Further quantitative analyses at the generic and specific levels will allow for more accurate descriptions of phylogenetic characters and character states.

Functional Morphology

Some of the functional attributes of the elements and the differences among groups have already been discussed, but the stance and locomotor patterns within Ceratopsia remain to be addressed.

Psittacosaurids have previously been determined to be bipedal based on limb proportions and the loss of manus digits (Osborn, 1923; Maryańska and Osmólska, 1975; Sereno, 1990). Several characteristics of the forelimbs of this group support this hypothesis, or at least suggest a different functional complex than that seen in neoceratopsians. The *Psittacosaurus* humerus is more robust than those of the basal neoceratopsians, and the deltopectoral crest extends farther laterally. The lateral position of the deltopectoral crest is associated with the partially sprawling position (and weight-bearing) of the element in neoceratopsians. In some of the basal neoceratopsians (i.e., TCM 2001.96.4) this crest extends much farther ventrally (caudally; it wraps around from the side of the element with the head to the back) than in *Psittacosaurus*, suggesting a more upright position of the forelimbs of TCM 2001.96.4 (Chinnery, pers. obs.). However, the more robust deltopectoral crests of *Psittacosaurus* indicate relatively large deltoid and/or pectoralis muscles, tentatively indicating an alternate functional use of the forelimb in this taxon. Supporting this interpretation, in addition to the crest size, is the observation that the *Psittacosaurus* humeral head and corresponding glenoid fossa on the scapulocoracoid are both larger than those of basal neoceratopsians. This suggests that the shoulder experienced a greater load than in the basal neoceratopsians with their smaller, less congruent, shoulder joints. The *Psittacosaurus* radius is more robust than in basal neoceratopsians and has a more rounded proximal end, suggesting the possibility of increased mobility (full rotation of the forelimb is not being suggested here, but maybe a more movable manus and forelimb than seen in basal neoceratopsians) and thus some form of manipulation of the environment different from what the neoceratopsians were doing.

The pelvis of *Psittacosaurus* exhibits traits that suggest either a difference in stance or in locomotion from that of neoceratop-

TABLE 1. Evolutionary trends in ceratopsian postcranial elements, as they occur phylogenetically on the composite cladogram in Figure 1

Iternode	1	2	3	4
Scapula	Less robust, acromion less robust and shifted distally, distal shift of the ventral curve on the dorsal blade	More robust, greater height prox. and distally shorter, distal shift of ventral curve, larger glenoid, less laterally curved	Shorter shaft, laterally wider, less laterally curved, deeper ventral curve	
Coracoid	Longer caudal process, less pronounced rim, larger main body, larger and flatter in ventral view, less distance between rim and caudal process	Less distance between rim and caudal process, longer caudal process, larger foramen	Fossa is sharper and deeper and slightly smaller, smaller foramen	
Humerus	Less robust, taller and more rounded head, larger and more robust distal end	More robust, longer and larger DP crest, head larger and more lateral, ventral shift of distal end	More robust	DP crest well developed
Ulna		More robust, larger caudodistal corner, longer olecranon	More robust, larger proximal olecranon, expanded distal end, laterally wider across notch	
Radius	Less robust, proximal end shifted laterally, most ventral point more medial	More robust, more expansion of ends, most ventral point is more medial, expansion of proximomedial corner	Slightly more robust, the most ventral point is more medial, proximomedial and distolateral corners expanded	Flattened proximal end
Ilium	Taller through peduncles, more narrow pubic peduncle, pubic peduncle less cranial	Shorter throughout, shorter pubic peduncle, ventral dip of the dorsal border is more cranial, highest point is more cranial	More ventrally curved, shorter pre-and postacet. blades, more cranial peduncles, larger acetabulum, more lateral width, shorter lateral overhang	Preacetabular blade more ventrally located
Ischium		Greater curvature, shorter through iliac peduncles, larger articular area	More robust, more curved, proximal shaft curves dorsally	Peduncles pinched together, peduncles wider, shorter shaft
Pubis		Reduction of pubic body and extension of prepubis, shorter iliac peduncle	Taller prepubis, most ventral point of dorsal border is more proximal	
Femur	Wider proximal end, shorter gr. trochanter, more narrow distal end, shorter distal articular area	Taller head, taller greater trochanter, more distal cranial trochanter, longer articular area	More robust, proximally wider, taller head, medial condyle extends further distally	Short femoral head
Tibia	Proximal end wider and taller, astragalar facet wider and taller, calcaneal facet more narrow	More robust, especially medially, astragalar facet is taller medially, wider calcaneal facet	More robust, more narrow proximally in cranial view, distally wider, calcaneal facet wider	
Fibula	Wider proximally and at midshaft, more narrow distally	More robust, taller articular ends, medial shift of proximal end	More robust but more narrow distal end, taller articular ends	

sians. The pubic peduncle of the ilium is located farther cranially, both articular processes of the ischium are more cranially oriented, and the acetabulum is smaller. If psittacosaurs were facultatively bipedal, one would expect the pelvis to be rotated caudoventrally, the acetabulum to be located farther cranially and more bone mass farther caudally in the pelvis, all to accommodate the difference in center of gravity. These differences suggest that this was the case, and argue for the bipedal stance of the group.

The pelvic traits of *Psittacosaurus* support the hypothesis of bipedality in this group, and the forelimb traits discussed above may therefore be interpreted as a functional complex for some form of manipulation of the environment such as reaching for plants.

Bipedality in basal neoceratopsians has been suggested by the more ventrocaudally projecting deltopectoral crest of the humerus as well as limb proportions (hind limb elements relatively longer than the forelimb elements; Maryańska and Osmólska, 1975). However, the deltopectoral crest does not project caudally in *Psittacosaurus*, suggesting that this character is insufficient to determine bipedality. Other interpretations for the orientation of the deltopectoral crest follow. The radius of basal neoceratopsians is less mobile, and none of the manus and pelvic traits discussed above for *Psittacosaurus* is present. In contrast, the broad, robust manus and straight femur of basal neoceratopsians argue against bipedality (caudodistally recurved femora are found in many archosaurian bipeds; Russell, 1970). The only basal form that exhibits postcranial traits similar to those of *Psittacosaurus* is *Udanoceratops*, which has a radius with a broad, flat head and a tall ilium. *Udanoceratops* also exhibits many other postcranial characters that are unique among basal neoceratopsians, and, because the skeleton is incompletely known, the locomotor patterns of this genus are unclear.

A large shift in body size accompanies the characters separating basal neoceratopsians and ceratopsids. Stance may have differed among neoceratopsians, with the forelimbs of basal neoceratopsians more upright in position than those of ceratopsids, as is suggested by the ventrally projecting deltopectoral crests in the former. In addition, the more lateral position of the ceratopsid humeral head and the ventral shift of the distal end of the element suggest that it was held more horizontally and laterally than in the basal neoceratopsians. A more horizontal humerus would explain the taller olecranon process on the ceratopsid ulna, as well, because the triceps muscles would need to be

strong to keep the elbow in extension and to bear the weight of the animal, with possibly a corresponding increase in size of the muscle attachment site on the olecranon. Results of the PCA in this study (Fig. 4J) support at least a correspondence of olecranon process size and overall size in ceratopsians, but it should be noted that size of the olecranon process does not correspond to sprawling or non-sprawling stance in other groups (i.e., crocodilians have small olecranon processes and stegosaurs [non-sprawlers] have tall ones; Carpenter, pers. comm.). Ceratopsid forelimb position has been debated for decades, with interpretations of posture ranging from sprawling with the humerus almost horizontal (Gilmore, 1905; Sternberg, 1927; Lull, 1933) to almost fully erect (Bakker, 1987; Paul, 1991). A sprawling posture seems to be inherent in the articulations of the pectoral girdle to the humerus (Osborn, 1933; Johnson and Ostrom, 1995; Dodson and Farlow, 1997), whereas footprints suggest a more upright stance (Lockley and Hunt, 1995). Dodson and Farlow (1997) suggested an inclined ulna and radius along with a partially sprawling humerus, accounting for the discrepancy. My results indicate a partially sprawling humerus, a result intermediate between the above studies apart from Dodson and Farlow (1997): consistent with the results obtained from the one-eighth-size model of *Triceratops* in the Virtual *Triceratops* Project at the USNM (Chapman et al., 1999). Most likely, the humerus changed positions during the gait cycle, with the element more upright at the ends of the cycle and more sprawling as the leg was brought around from back to front during the cycle (Chapman et al., 1999).

The neoceratopsian hindlimb exhibits changes primarily associated with increase in size and weight, but the limbs appear to bow out laterally more as size increases, an unexpected trend (mechanically, limbs would be expected to become more columnar with increasing weight, as they do in extant large mammals). Characters supporting this observation include the greater increase in lateral condyle size versus that of the medial condyle, lateral bowing of the femur itself, and an increase in femoral head height with size. In the tibia, the lateral side of the distal end of the element expands at a much greater rate than the medial side, perhaps to accommodate the greater amount of weight placed here due to the lateral bowing of the limb. Although counterintuitive, this trend has been noted previously (Paul, 1991) and is most likely due to a relative increase in abdomen size with overall increase in size. A comparable trend is seen in titanosaurid limb posture, and is similarly interpreted (Wilson and Carrano, 1999).

SUMMARY

Ceratopsian girdle and limb elements increased in robustness through Neoceratopsia and within Psittacosauridae. The majority of the measurements increased with positive allometry compared to length of the elements. The ventral scapulocoracoid, distal humerus, proximal ulna, proximal and distal ends of the radius, prepubic process, distal femur, distal tibia, and proximal and distal ends of the fibula reflect this the most. Some measurements increased with negative allometry, while still providing evidence for increasing robustness. These include the length from the rim of the sigmoid fossa of the ulna distally, length of the postacetabular process of the ilium, all height measurements of the ilium, and height of the articular portion of the pubis. Some measurements that would be assumed to show allometric trends change nearly isometrically with increasing length, including maximum height of the scapula, deltopectoral crest length of the humerus, and width of the femoral shaft at 75% length.

The plesiomorphic condition of bipedality in *Psittacosaurus* is supported by the shape comparisons. Indicators of bipedality and possible alternate forelimb use in *Psittacosaurus* as contrasted to neoceratopsians include a more mobile radial head, reduced manus digits, and modifications of the pelvis that support more weight cranially. Forelimb elements of *Psittacosaurus* are more robust than those of basal neoceratopsians, and this trend, together with increased mobility, suggests that their forelimbs were used for manipulation of the environment in some way. The shift to quadrupedalism in basal neoceratopsians is verified by the change in orientation of the deltopectoral crest on the humerus, the more compact manus, and the shift in the pelvic elements to support more weight centrally.

The increase in size from the basal neoceratopsians to ceratopsids is reflected in a change of stance from the more upright one of the basal neoceratopsians to a more sprawling posture, especially in the forelimbs. The deltopectoral crest is oriented more horizontally in ceratopsids, the olecranon process of the ulna is larger, and the lateral condyle of the femur and lateral side of the distal tibia are more developed.

The morphometric methods applied to this material complement and allow for control of each other. Each method provides certain information and allows for certain conclusions. Observations and results interpreted from a combination of all methods are more robust, closer to being unbiased, and are more informative than those formed from any one method.

ACKNOWLEDGMENTS

I thank the faculty and students of the Functional Anatomy and Evolution Program at the Johns Hopkins University School of Medicine for their help, encouragement and support through my graduate school years. I also thank the many people who helped me with this project, especially my thesis committee members Dave Weishampel, Ken Rose, Ralph Chapman, Peter Dodson, and Cathy Forster. Curators and collections managers at the museums where I collected data are too numerous to list; please accept my apologies and my thanks for all of your help. This project is part of the doctoral thesis of the author, and would not have been possible without grant money provided by the Society of Vertebrate Paleontology, the Jurassic Foundation, the Geological Society, and the Paleontological Society.

LITERATURE CITED

Adams, D. 1987. The bigger they are, the harder they fall: implications of ischial curvature in ceratopsian dinosaurs; pp. 1–6 in P. J. Currie and E. H. Koster (eds.), Fourth Symposium on Mesozoic Terrestrial Ecosystems. Occasional Paper of the Tyrrell Museum of Palaeontology 3.

Adams, D. 1991a. The significance of sternal position and orientation to reconstruction of ceratopsid stance and appearance. Journal of Vertebrate Paleontology 11(3, Supplement):14A.

Adams, D. 1991b. A scaling equation for humeral diameter in ceratopsian dinosaurs. The Texas Journal of Science 43:3–11.

Bakker, R. T. 1987. The return of the dancing dinosaurs; pp. 39–69 in S. J. Czerkas and E. C. Olson (eds.), Dinosaurs Past and Present, Volume I. Natural History Museum of Los Angeles County and University of Washington Press, Seattle.

Benson, R. H., R. E. Chapman, and A. F. Siegel. 1982. On the measurement of morphology and its change. Paleobiology 8:328–339.

Bookstein, F. L. 1991. Morphometric Tools for Landmark Data: Geometry and Biology. Cambridge. Cambridge University Press, 435 pp.

Brown, B. and E. M. Schlaikjer. 1940. The structure and relationship of *Protoceratops*. Annals of the New York Academy of Sciences 40: 135–266.

Chapman, R. E. 1990. Shape analysis in the study of dinosaur morphology; pp. 21–42 in K. Carpenter and P. J. Currie (eds.), Dinosaur Systematics - Approaches and Perspectives. Cambridge University Press, New York.

Chapman, R. E., P. M. Galton, J. J. Sepkoski, Jr., and W. P. Wall. 1981. A morphometric study of the cranium of the cranium of the pachycephalosaurid dinosaur *Stegoceras*. Journal of Paleontology 55: 608–618.

Chapman, R. E., and M. K. Brett-Surman. 1990. Morphometric observations on hadrosaurid ornithopods; pp. 163–177 in K. Carpenter and

P. J. Currie (eds.), Dinosaur Systematics. Cambridge University Press, Cambridge.
Chapman, R. E., D. B. Weishampel, G. Hunt, and D. Rasskin-Gutman. 1997. On using the shapes of dinosaurs. Dinofest International 1997: 31–37.
Chapman, R. E., A. F. Andersen, and S. J. Jabo. 1999. Construction of the virtual *Triceratops*: procedures, results, and potentials. Journal of Vertebrate Paleontology 19(3, Supplement):37A.
Chinnery, B. J. 2002. Morphometric analysis of evolution and growth in the ceratopsian postcranial skeleton. Unpublished Ph.D. dissertation, Johns Hopkins University School of Medicine, Baltimore, 360 pp.
Chinnery, B. J., and R. E. Chapman. 1998. A morphometric study of the ceratopsid postcranial skeleton. Journal of Vertebrate Paleontology 18(3, Supplement):33A.
Chinnery, B. J., and D. B. Weishampel. 1998. *Montanoceratops cerorhynchus* (Dinosauria: Ceratopsia) and relationships among basal neoceratopsians. Journal of Vertebrate Paleontology 18:569–585.
Dawson, S. D. 1994. Allometry of cetacean forelimb bones. Journal of Morphology 222:215–221.
Dodson, P. 1975a. Taxonomic implications of relative growth in lambeosaurine hadrosaurs. Systematic Zoology 24:37–54.
Dodson, P. 1975b. Functional and ecological significance of relative growth in *Alligator*. Journal of Zoology, London 175:315–355.
Dodson, P. 1976. Quantitative aspects of relative growth and sexual dimorphism in *Protoceratops*. Journal of Paleontology 50:929–940.
Dodson, P. 1980. Comparative osteology of the american ornithopods *Camptosaurus* and *Tenontosaurus*. Memoirs of the Society of Geology, France 139:81–85.
Dodson, P. 1990. On the status of the ceratopsids *Monoclonius* and *Centrosaurus*; pp. 231–244 in K. Carpenter and P. Currie (eds.), Dinosaur Systematics: Perspectives and Approaches. Cambridge University Press, Cambridge.
Dodson, P. 1993. Comparative craniology of the Ceratopsia; pp. 200–234 in P. Dodson and P. Gingerich (eds.), Functional Morphology and Evolution. American Journal of Science Special Volume 293-A.
Dodson, P. 1996. The Horned Dinosaurs. A Natural History. New Jersey: Princeton University Press, 360 pp.
Dodson, P., and P. J. Currie. 1990. Neoceratopsia; pp. 393–398 in D. B. Weishampel, P. Dodson, and H. Osmólska (eds.), The Dinosauria. University of California Press, Berkeley.
Dodson, P., and J. O. Farlow. 1997. The forelimb carriage of ceratopsid dinosaurs. Dinofest International Proceedings, 1997, pp. 393–398.
Dodson, P., C. A. Forster, and S. D. Sampson. In press. Ceratopsidae; in D. B. Weishampel, P. Dodson, and H. Osmólska (eds), The Dinosauria. University of California Press, Berkeley.
Dong, Z. and Y. Azuma. 1997. On a primitive neoceratopsian from the Early Cretaceous of China; pp. 68–89 in Z. Dong (ed.): Sino-Japanese Silk Road Dinosaur Expedition. China Ocean Press, Beijing.
Forster, C. A. 1990. The cranial morphology and systematics of *Triceratops*, with a preliminary analysis of ceratopsian phylogeny. Unpublished Ph.D. dissertation, University of Pennsylvania, Philadelphia, 227 pp.
Forster, C. A. 1996. New information on the skull of *Triceratops*. Journal of Vertebrate Paleontology 16:246–258.
Gilmore, C. W. 1905. The mounted skeleton of *Triceratops prorsus*. Proceedings of the U.S. National Museum 29:433–435.
Gilmore, C. W. 1917. *Brachyceratops*, a ceratopsian dinosaur from the Two Medicine Formation of Montana with notes on associated reptiles. United States Geological Survey Professional Paper 103:1–45.
Gray, S. W. 1946. Relative growth in a phylogenetic series and in an ontogenetic series of one of its members. American Journal of Science 244:792–807.
Hatcher, J. B., O. C. Marsh, and R. S. Lull. 1907. The Ceratopsia. U. S. Geological Survey, Monograph 491-XXIX:1–300.
Hughes, N. C. and R. E. Chapman. 1995. Growth and variation in the Silurian proetide trilobite *Aulacopleura konincki* and its implications for trilobite palaeobiology. Lethaia 28:333–353.
Huxley, J. S. 1932. Problems of Relative Growth. New York, Dover Publications, 302 pp.
Johnson, R. E. and J. H. Ostrom. 1995. The forelimb of *Torosaurus* and an analysis of the posture and gait of ceratopsians; pp. 205–218 in J. Thomason (ed.), Functional Morphology in Vertebrate Paleontology. Cambridge University Press, Cambridge.
Jolicoeur, P. and J. E. Mosimann. 1960. Size and shape variation in the painted turtle. A principal components analysis. Growth 24:339–354.
Lehman, T. M. 1989. *Chasmosaurus mariscalensis*, n. sp. a new ceratopsian dinosaur from Texas. Journal of Vertebrate Paleontology 9: 137–162.
Lehman, T. M. 1990. The ceratopsian subfamily Chasmosaurinae: sexual dimorphism and systematics; pp. 211–230 in K. Carpenter and P. Currie (eds.), Dinosaur Systematics: Perspectives and Approaches. Cambridge University Press, Cambridge.
Lele, S. 1991. Some comments on coordinate-free and scale-invariant methods in morphometrics. American Journal of Physical Anthropology 85:407–417.
Lele, S., and T. M. Cole. 1996. A new test for shape differences when variance-covariance matrices are unequal. Journal of Human Evolution 31:193–212.
Lele, S., and J. T. Richtsmeier. 1991. Euclidean Distance Matrix Analysis: A coordinate-free approach for comparing biological shapes using landmark data. American Journal of Physical Anthropology 86: 415–427.
Lockley, M. G., and A. P. Hunt. 1995. Ceratopsid tracks and associated ichnofauna from the Laramie Formation (Upper Cretaceous: Maastrichtian) of Colorado. Journal of Vertebrate Paleontology 15: 592–614.
Lull, R. S. 1933. A revision of the Ceratopsia or horned dinosaurs. Peabody Museum of Natural History Memoirs 3:1–175.
Lull, R. S., and S. W. Gray. 1949. Growth patterns in the Ceratopsia. American Journal of Science 247:492–503.
Makovicky, P. J. 2001. A *Montanoceratops cerorhynchus* (Dinosauria: Ceratopsia) braincase from the Horseshoe Canyon Formation of Alberta; pp. 243–262 in D. H. Tanke and K. Carpenter (eds.), Mesozoic Vertebrate Life. Indiana University Press, Bloomington.
Makovicky, P. J. 2002. Taxonomic revisions and phylogenetic relationships of basal Neoceratopsia (Dinosauria: Ornithischia). Unpublished Ph.D. dissertation, Columbia University, 288 pp.
Maryańska, T. 1990. Pachycephalosauria; pp. 564–577 in D. B. Weishampel, P. Dodson, and H. Osmólska (eds.): The Dinosauria. University of California Press, Berkeley.
Maryańska, T., and H. Osmólska. 1974. Pachycephalosauria, a new suborder of ornithischian dinosaurs. Palaeontologica Polonica 30: 45–102.
Maryańska, T., and H. Osmólska. 1975. Protoceratopsidae (Dinosauria) of Asia. Palaeontologica Polonica 33:133–182.
Osborn, H. F. 1923. Two Lower Cretaceous dinosaurs of Mongolia. American Museum Novitates 95:1–3.
Osborn, H. F. 1933. Mounted skeleton of *Triceratops elatus*. American Museum Novitates 654:1–14.
Ostrom, J. H., and P. Wellnhofer. 1986. The Munich specimen of *Triceratops* with a revision of the genus. Zitteliana 14:111–158.
Oxnard, C. E. 1978. Primate quadrupedalism: some subtle structural correlates. Yearbook of Physical Anthropology 20:538–554.
Oxnard, C. E. 1983. Anatomical, biomolecular and morphometric views of the primates. Progress in Anatomy 3:113–142.
Oxnard, C. E. 1984. The place of *Tarsius* as revealed by multivariate statistical morphometrics; pp. 17–32 in C. Niemitz (ed.), Biology of Tarsiers. Fischer Verlag, Tubingen.
Paul, G. S. 1991. Giant horned dinosaurs did have fully erect forelimbs. Journal of Vertebrate Paleontology 11(3, Supplement):50A.
Reyment, R. A., R. E. Blackith, and N. A. Campbell. 1984. Multivariate Morphometrics, 2nd edition. Academic Press, London, 233 pp.
Richtsmeier, J. T., J. M. Cheverud, and S. Lele. 1992. Advances in anthropological morphometrics. Annual Review of Anthropology 21: 283–305.
Rohlf, F. J. 1998. TPS Dig computer program, Stony Brook, New York.
Rohlf, F. J., and D. Slice. 1990. Extensions of the Procrustes method for the optimal superimposition of landmarks. Systematic Zoology 39: 40–59.
Romer, A. S. 1956. Osteology of the Reptiles. Chicago, University of Chicago Press, 772 pp.
Russell, D. A. 1970. A skeletal reconstruction of *Leptoceratops gracilis* from the upper Edmonton Formation (Cretaceous) of Alberta. Canadian Journal of Earth Sciences 7:181–184.
Sampson, S. D., M. J. Ryan, and D. H. Tanke. 1997. Craniofacial ontogeny in centrosaurine dinosaurs (Ornithischia;Ceratopsidae): taxonomic and behavioral implications. Zoological Journal of Linnean Society 121:293–337.

Sereno, P. C. 1984. The phylogeny of the Ornithischia: a reappraisal; pp. 219–226 in W. Reif and F. Westfal (eds.), Third Symposium on Mesozoic Terrestrial Ecosystems, Short Papers. Attempto Verlag, Tubingen University Press, Tubingen.

Sereno, P. C. 1986. Phylogeny of the bird-hipped dinosaurs (Order Ornithischia). National Geographic Research 2:234–256.

Sereno, P. C. 1990. Psittacosauridae; pp. 579–592 in D. B. Weishampel, P. Dodson, and H. Osmólska (eds.), The Dinosauria. University of California Press, Berkeley.

Sereno, P. C. 2000. The fossil record, systematics and evolution of pacycephalosaurs and ceratopsians from Asia; pp. 480–516 in M. J. Benton, M. A. Shishkin, D. M. Unwin, and E. N. Kurochkin (eds.), The Age of Dinosaurs in Russia and Mongolia. Cambridge University Press, Cambridge.

Siegel, A. F., and R. H. Benson. 1982. A robust comparison of biological shapes. Biometrics 38:341–350.

Sternberg, C. M. 1927. Horned dinosaur group in the National Museum of Canada. Canadian Field-Naturalist 41:67–73.

Tereshchenko, V. S. 1991. The reconstruction of the vertebral column of *Protoceratops*. Paleontological Journal 2:86–96 (English 106–116).

Tereshchenko, V. S. 1994. A reconstruction of the erect posture of *Protoceratops*. Paleontological Journal 28:104–119.

Tereshchenko, V. S. 1996. A reconstruction of the locomotion of *Protoceratops*. Paleontological Journal 30:232–245.

Thompson, D. W. 1917. On Growth and Form. Cambridge, Cambridge University Press, 1116 pp.

Van Valkenburgh, B. 1987. Skeletal indicators of locomotor behavior in living and extinct carnivores. Journal of Vertebrate Paleontology 7:162–182.

Watabe, M. and H. Nakaya. 1991. Phylogenetic significance of the postcranial skeletons of the hipparions from Maragheh (Late Miocene), Northwest Iran. Memoirs of the Faculty of Science, Kyoto University, Series of Geology and Minerology LVI:11–53.

Weishampel, D. B. and R. E. Chapman. 1990. Morphometric study of *Plateosaurus* from Trossingen (Baden-Wurttemberg, Federal Republic of Germany); pp. 43–51 in K. Carpenter and P. J. Currie (eds.), Dinosaur Systematics: Perspectives and Approaches. Cambridge University Press, Cambridge.

Wilson, J. A. and M. T. Carrano. 1999. Titanosaurs and the origin of "wide-gauge" trackways: a biomechanical and systematic perspective on sauropod locomotion. Paleobiology 25:252–267.

Zhao, X., C. Zhengwu, and X. Xing. 1999. The earliest ceratopsian from the Tuchengzi Formation of Liaoning, China. Journal of Vertebrate Paleontology 19:681–691.

Received 2 December 2002; accepted 6 October 2003.

APPENDIX

Supplemental data available from SVP website: http://www.vertpaleo.org/jvp/JVPcontents.html.